

# Millimetre dust emission from northern Bok globules<sup>★</sup>

R. Launhardt and Th. Henning

Astrophysical Institute and University Observatory Jena, Schillergäßchen 2-3, D-07745 Jena, Germany (launh@astro.uni-jena.de)

Received 29 January 1997 / Accepted 28 April 1997

**Abstract.** We present the results of a 1.3 mm continuum study of 59 Bok globules located north of  $-30^\circ$  declination. The catalogue of Clemens & Barvainis (1988) served as a search list for the target objects investigated here. Based on the analysis of the IRAS point source colour-colour diagram, four distinct groups of globules are distinguished. It is shown that indeed each of these groups has distinctive properties and represents a different stage of star formation. For our observations, we selected a number of candidate pre-protostellar cores, all candidates for globules with protostellar cores, as well as a number of strong  $12\ \mu\text{m}$  IRAS point sources which are candidates for T Tauri stars associated with globules.

Individual distances of the globules are derived with a method which associates the globules with larger molecular cloud complexes. It is shown that most globules are associated with such cloud complexes from which they probably formed. The derived distances range from 140 pc to 2 kpc with the majority of the globules being related to Gould's Belt at distances of 200 to 300 pc. The average distance of our sample of globules is derived to be 500 pc.

Out of the 59 globule cores observed at 1.3 mm, 21 objects were detected with average  $3\sigma$  detection limits of 17 mJy/12'' and 39 mJy/23''. This corresponds to an overall detection rate of 35%. While most of the detected objects are protostellar cores, four pre-protostellar cores and one T Tauri star were detected furthermore. The typical mass of a star formed in a Bok globule is derived to be  $\approx 0.5 M_\odot$ . Using the detection rates and the relative frequencies of the globule groups, lifetimes of the different evolutionary stages are derived. Assuming that all globules form stars at some time of their evolution, the typical lifetime of a Bok globule is derived to be some  $10^6$  years. It is speculated that the existence of isolated T Tauri stars can be explained by star formation in Bok globules. In addition, the results of the continuum measurements are compared with observations of different molecular lines.

**Key words:** circumstellar matter – stars: formation – ISM: clouds – dust, extinction – radio continuum: ISM

*Send offprint requests to:* R. Launhardt

<sup>★</sup> Partially based on observations collected at the European Southern Observatory, La Silla, Chile

## 1. Introduction

The study of low-mass star formation is observationally more straightforward in small, nearby, and relatively isolated regions. They are free from the complicating effects of large numbers of newly-formed stars, with their associated stellar winds and outflows, which abound in regions such as Chamaeleon, Taurus, and Ophiuchus.

Bok globules, which are the most simple molecular clouds in our Milky Way, are perfectly suited to study the low-mass star formation process in detail, even if they are not a dominant constituent of the interstellar medium. They are small, opaque, and relatively isolated molecular clouds with diameters of 0.7 pc (0.1–2 pc) and masses of  $\approx 10 M_\odot$  (2–100  $M_\odot$ ) (see, e.g., Bok 1977, and Leung 1985 for reviews). Nearby globules appear as small patches of high obscuration against the star-rich background of the galactic plane. The total number of globules in our galaxy is estimated to be some  $10^5$  (Clemens et al. 1991, hereafter CYH91).

Several catalogues of dark clouds and globules were published during the past 20 years (e.g. Sandquist & Lindroos 1976; Feitzinger & Stuewe 1984; Hartley et al. 1986; Persi et al. 1990) most of which tend, however, to select preferentially larger clouds. The most homogeneous and complete compilation of northern globules is the ‘‘Catalog of small, optically selected molecular clouds’’ by Clemens & Barvainis (1988, hereafter C&B88, or CB catalogue). This catalogue contains 248 small dark clouds which were identified on the Palomar Observatory Sky Survey plates. It is, therefore, restricted to globules north of  $-30^\circ$  declination. The globules of the CB catalogue have angular diameters of less than  $10'$  (mean  $4'$ ), and mostly appear to be well isolated and opaque in their central regions.

The significance of such globules in the star formation process was first recognized by Bok and co-workers (e.g. Bok & Reilly 1947) who described them, for the first time, as a distinct group of astronomical objects. Recent studies of isolated globules demonstrated that, indeed, at least a fraction of these clouds are active sites of low-mass star formation (e.g. Reipurth 1983; Neckel et al. 1985; C&B88; CYH91; Yun & Clemens 1992; Zhou et al. 1993; Launhardt & Henning 1994; Bourke et al. 1997), whereas others seem to be rather quiet and stable (Dickman & Clemens 1983).

C&B88 listed all of the known IRAS Point Source Catalog (PSC) associations with the globules. They found 109 globules (44% of the sample) to have IRAS point sources within their boundaries (“core type” sources) indicating the presence of centrally condensed cores or embedded young stellar objects (YSOs). Observations in molecular lines showed that globules are, indeed, cold molecular clouds ( $T_{\text{kin}} \approx 10$  K) which often have dense cores (see, e.g., Martin & Barrett 1978; CYH91; Lemme et al. 1996; Wang et al. 1997). These dense cores are the sites where new stars are presently formed or they may even represent the protostars themselves. In fact, in some of these dense cores, spectroscopic evidence of protostellar collapse was found (Zhou et al. 1993; Wang et al. 1995, 1997). Further indication of ongoing star formation comes from the detection of 14 molecular outflows in a sample of 41 northern globules by Yun & Clemens (1992) and of 11 molecular outflows in a sample of 35 southern globules by Henning & Launhardt (1997).

Despite of the large number of studies during the last years, there is little known about the incidence and the properties of such dense cores in Bok globules. A basic problem of spectral line observations towards cold dense cores is the fact that most of the easily observable spectral lines get opaque in regions of high column densities. Many molecules may also freeze out on the dust grains in these cold cores at densities of  $n_{\text{H}} > 10^6 \text{ cm}^{-3}$  (see, e.g., Mezger et al. 1992; Blake et al. 1994). The thermal mm dust emission, on the other hand, remains optically thin in these regions and, thus, provides an excellent tracer of protostellar cores and dense circumstellar material around the newly born stars. In addition, it yields reliable estimates of hydrogen column densities and masses.

In this paper, we present the results of the first systematic study of the 1.3 mm dust continuum emission from Bok globules. We describe the selection criteria for our target list (Sect. 2), the observing procedure and data reduction (Sect. 3), and determine the individual distances towards the globules (Sect. 4). The results of this survey are presented in Sect. 5 and discussed in Sect. 6.

## 2. Classification, selection criteria and source list

For our 1.3 mm continuum study, the CB catalogue served as a search list. Our target list is, therefore, restricted to globules north of  $-30^\circ$  declination. Since our observations were mainly focussed on the identification of star-forming cores among the globules, the major selection criteria were the presence of “cold” IRAS point sources (far-infrared colour temperature  $T_{\text{FIR}} < 40$  K) and a high visual extinction. The FIR colour temperature  $T_{\text{FIR}}$  is calculated here from the 60 and  $100 \mu\text{m}$  IRAS point source fluxes and is corrected for the dust emissivity index ( $\beta = 1.8$ , see Sect. 5). For the characterization of the dense cores (typical angular diameter  $1'$  or less), the IRAS point source fluxes have to be used rather than the co-added IRAS fluxes because the latter ones include the extended emission from the entire globule (diameter of a few arcminutes) and not only the emission from the dense cores. In the following, the

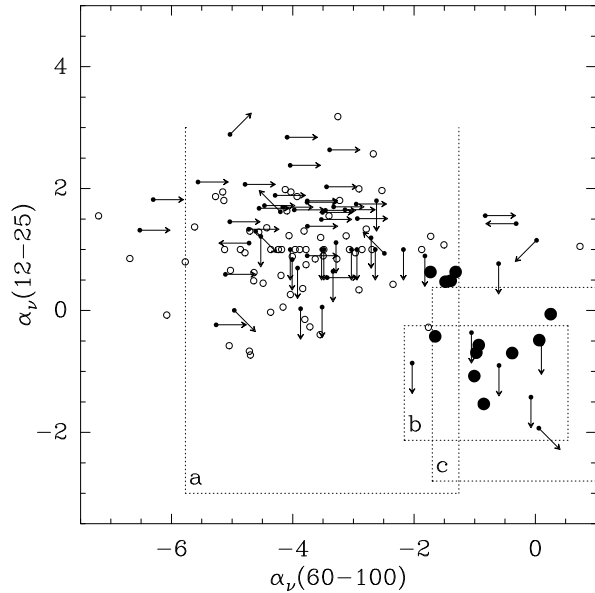


**Fig. 1.** IRAS colour-colour diagram for all core-type IRAS point sources in CB globules. Sources with valid fluxes in all four IRAS bands are marked by large filled circles. Sources for which none of the colour indices is reliable due to upper flux limits are marked by open circles. Sources which only have a valid  $\alpha_\nu(12-25)$  or  $\alpha_\nu(60-100)$  index are indicated by horizontal or vertical arrows, respectively, showing the direction of the shift in the diagram. For the sake of comparison, the areas of different object classes are marked in the colour-colour plane by rectangular boxes: (a) Cirrus clouds (Meurs & Harmon 1988), (b) dense molecular cloud cores (Emerson 1987), (c) IRAS outflow cloud cores (Morgan & Bally 1991; Wouterloot et al. 1989)

selection criteria for the IRAS point sources will be explained more specifically.

In order to characterize the infrared (IR) broad-band spectral energy distributions (SEDs) and to quantify the IRAS flux ratios, we used the IR spectral index  $\alpha_\nu$  which was introduced by Lada (1987; see also Wilking et al. 1989):

$$\alpha_\nu(\lambda_1 - \lambda_2) = \frac{\lg[S_\nu(\lambda_1)/\lambda_1] - \lg[S_\nu(\lambda_2)/\lambda_2]}{\lg[\lambda_2] - \lg[\lambda_1]} \quad (1)$$

where  $S_\nu(\lambda_i)$  is the flux density in Jy at the wavelength  $\lambda_i$  in  $\mu\text{m}$ . According to the definition of  $\alpha_\nu$ , the colour temperature increases with increasing colour indices. While the mid- to near-IR SED characterizes the hot dust in the immediate vicinity of the YSO (e.g. the inner disk), the FIR SED rather characterizes the outer disk or the colder dust in the dense core.

Only a small fraction of the globule cores has valid flux measurements (no upper limits) in all 4 IRAS bands. While many objects are too cold to be detected by IRAS at mid-IR wavelengths, others do not have enough cold dust to be detected at long wavelengths. In total, only 20% of the IRAS sources associated with CB globules have valid fluxes in three or all four bands. Fig. 1 shows the location of all “core-type” IRAS point sources in the IRAS colour-colour diagram.

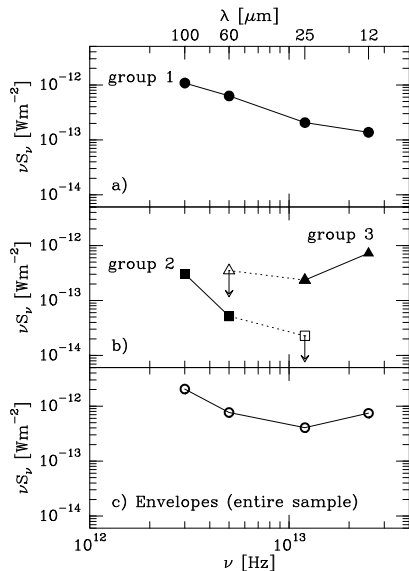


**Fig. 2a–c.** Broad-band SEDs averaged over all members of the individual groups for **a** group 1, **b** group 2 (squares) and group 3 (triangles). Upper limits are marked by open symbols and down-arrows. **c** Co-added IRAS fluxes (CYH91) minus point source IRAS fluxes averaged over the entire sample.

The colour-colour diagram (Fig. 1) clearly reveals that the entire sample of IRAS point sources in globules breaks up into two main groups: one with  $\alpha_\nu(60 - 100) \geq -2.3$  and one with  $\alpha_\nu(60 - 100) < -2.3$ . All sources of the second group have upper flux limits in at least one and up to three bands. Therefore, at least one of the two colour indices of these sources represents the detector properties or the background emission rather than the source properties. Depending on the wavelength bands in which the sources were detected, the second group can be further subdivided.

In order to simplify the understanding of the target selection and the interpretation of the data, we subdivided the CB globules into different object groups according to the properties of their associated IRAS point sources. In addition, we compiled the averaged broad-band SEDs of the groups from the IRAS point source fluxes (Fig. 2). We will later show that indeed each of these groups has distinctive properties and represents a different evolutionary stage of star formation. We introduce here the following groups of globules:

- *Group 1:* Sources which were at least detected at 60 and 100  $\mu\text{m}$  and which have  $\alpha_\nu(60 - 100) \geq -2.3$  (20 globules). These sources have a mid-IR colour index of  $\alpha_\nu(12 - 25) < 1$ . Their SEDs are steadily rising from 12 to 100  $\mu\text{m}$ , but they are much broader than that of a single-temperature blackbody. The FIR spectral index range of this group translates into colour temperatures between 25 and 35 K. It should be noted that all sources of the sample which have 4 valid IRAS point source flux measurements belong to this group. The location of these sources in the colour-colour diagram (Fig. 1) compares to the location of

other star-forming molecular cloud cores (Emerson 1987) and IRAS outflow sources (Morgan & Bally 1987). They are, therefore, good candidates for internally heated star-forming cloud cores (protostellar cores).

- *Group 2:* Sources which were at least detected at 100  $\mu\text{m}$  and which have  $\alpha_\nu(60 - 100) < -2.3$  if they were also detected at 60  $\mu\text{m}$  (40 globules). Their SEDs are steeply rising from 60 to 100  $\mu\text{m}$  ( $T_{\text{FIR}} \approx 19$  K). The FIR fluxes are extremely low compared to other objects and are close to the detection limit of IRAS. No emission short-ward of 60  $\mu\text{m}$  was detected and no molecular outflow has been found so far towards one of these sources. These objects are, therefore, candidates for pre-protostellar cores (Ward-Thompson et al. 1994) or extremely young protostellar cores (“Class -I”, Boss & Yorke 1995). It can, however, not be excluded that especially the less opaque globules in this group are simply cirrus regions (see Fig. 1).
- *Group 3:* Sources which were at least detected at 12  $\mu\text{m}$ , which have  $-0.5 < \alpha_\nu(12 - 25) < 3$ , and which were not detected at 100  $\mu\text{m}$  (32 globules). In contrast to the objects of group 1 and 2, the group 3 sources radiate no energy at FIR wavelengths, but have SEDs which are rising towards shorter wavelengths. We speculate, therefore, that these objects are candidates for much more evolved young stars which still have a considerable amount of hot circumstellar dust.
- *Group 4:* All globules which have no associated “core-type” IRAS point sources (139 globules).

A remainder of 17 globules could not be classified within this scheme. Fig. 2 shows clearly that the SEDs of the three groups of embedded sources differ strongly from each other. There is no such systematic difference between the SEDs of the extended envelopes, which were compiled from the co-added IRAS fluxes (CYH91) after subtraction of the associated point source fluxes (emission of the entire globule minus contribution from the embedded sources). For this reason, Fig. 2c shows only one average envelope SED for the entire sample.

For the mm continuum observations, we selected 19 out of the 20 globules of group 1. CB 199 (B 335) which also belongs to this group was not included in our study because this globule is already well investigated by other authors (e.g. Keene et al. 1983; Gee et al. 1985; Chandler et al. 1990; Zhou et al. 1993). Five globules were selected from group 2 to search for the youngest star-forming cores. In order to include young stars which were already formed in the globules, we selected 15 globules of group 3. Opaque globules and sources with high 12  $\mu\text{m}$  fluxes ( $S_{12} > 1$  Jy) were preferentially selected and large globules which are part of more complex dark clouds were, in general, excluded. Four other opaque globules which are associated with IRAS point sources which cannot be classified within this scheme were added to our source list (indicated by “?” in Table 1). In addition, we selected 15 small, opaque, and isolated globules of group 4 which have no associated IRAS point sources in order to search for pre-protostellar cores.

In total, we selected 59 globules from the CB catalogue of which 44 globules have one or more IRAS point sources within

**Table 1.** Coordinates and distances of the selected globules

Name	Group	IRAS Name	RA(1950) (h m s)	Dec(1950) (° ' ")	Other names	<i>D</i> (pc)	Association, Method	References, Remarks	Reliability class
CB 3	1	00259+5625	00 25 59.0	56 25 32	LBN594	2500	I, b	1, 3, 17	B
CB 6	1	00465+5028	00 46 34.3	50 28 25	LBN613	800	II	1, 19	B
CB 12	2	01354+6447	01 35 24.3	64 47 59	—	800	II	1, 19	B
CB 17	2	04005+5647	04 00 30.8	56 47 59	L1389	300	III	1, 6, 18	B
CB 22	4	—	04 37 25.0	29 48 57	L1503, B23	140	IV	1, 2	A
CB 23	4	—	04 40 22.0	29 34 26	L1507	140	IV	1, 2	A
CB 26	1	04559+5200	04 55 56.1	52 00 17	L1439	300	III	1, 6, 18	B
CB 34	1	05440+2059	05 44 02.8	20 59 07	—	1500	V	1, 5	A
CB 39	1	05591+1630	05 59 06.0	16 30 58	(HD250550)	1500	V	1, 5	A
CB 45	4	—	06 06 00.0	17 50 52	L1578	1500	V	1, 5	A
CB 52	1	06464–1650	06 46 25.3	–16 50 38	—	1500	b, (VI)	3, 7	B
CB 54	1	07020–1618	07 02 06.0	–16 18 47	LBN1042	1500	b, (VI)	3, 7	B
CB 58-2	1	07161–2336	07 16 09.1	–23 36 11	—	1500	b, (VI)	3, 7	B
CB 60-1	1	08026–3122	08 02 38.2	–31 22 09	L1670	1500	b, VIII	3	B
CB 67	3	16482–1906	16 48 14.2	–19 06 11	L31	160	VII	1, 8	A
CB 68	1	16544–1604	16 54 27.2	–16 04 48	L146	160	VII	1, 8	A
CB 69-2	3	16595–3311	16 59 31.1	–33 11 15	B49	500	a		C
CB 78	4	—	17 14 23.0	–18 28 21	L173, B64	160	VII	1, 8	A
CB 80	4	—	17 18 50.0	–21 45 31	L1774	160	VII	1, 8	A
CB 81	?	17193–2705	17 19 22.9	–27 05 56	L1774	160	VII	1, 8	A
CB 82	3	17194–2351	17 19 28.1	–23 51 00	L55, B68	160	VII	1, 8, 4	A
CB 92	4	—	17 37 47.0	–19 38 21	L226	160	c, (VII)	1	B
CB 95	4	—	17 42 23.0	–19 59 20	L233, B83	160	c, (VII)	1	B
CB 97-2	3	17438–2017	17 43 52.8	–20 17 45	L235, B84	160	c, (VII)	1	B
CB 98	4	—	17 44 02.0	–20 29 26	—	160	c, (VII)	1	B
CB 107-1	3	17597–2754	17 59 43.3	–27 54 37	L93, B86	180	XVII	1	B
CB 107-2	3	17597–2749	17 59 45.4	–27 49 44	—	—	—	—	—
CB 108	3	18001–2023	18 00 07.1	–20 53 07	L262	180	XVII	1	B
CB 110	3	18032–1826	18 03 15.0	–18 26 51	L307	180	XVII	1	B
CB 114	3	18093–2241	18 09 18.6	–22 41 23	—	180	XVII	1	B
CB 116-2	3	18095–2246	18 09 30.1	–22 46 54	—	180	XVII	1	B
CB 125-2	3	18127–1803	18 12 46.6	–18 03 37	L323, B92	200	XVII	1, 4	B
CB 126	4	—	18 12 39.0	–03 46 38	L490	200	IX	1	A
CB 130	4	—	18 13 38.0	–02 33 52	L507	200	IX	1	A
CB 131	4	—	18 14 04.0	–18 03 52	L328, B93	180	XVII	1	B
CB 135-1	2	18203–2047	18 20 22.6	–20 47 21	L306	180	XVII	1	B
CB 138	?	18221–1055	18 22 09.4	–10 55 11	L414	200	IX	1	A
CB 139	?	18225–1043	18 22 31.8	–10 43 13	L416, B94	200	IX	1	A
CB 142	3	18272–1343	18 27 12.1	–13 43 12	—	500	a		C
CB 143	3	18274–1743	18 27 28.5	–17 43 16	L356, B311	180	XVII	1	B
CB 145	3	18296–0911	18 29 37.2	–09 11 40	L443, B100	200	IX	1	A
CB 155-1	3	18445–0440	18 44 35.9	–04 40 42	B104	200	IX	1	A
CB 155-2	3	18446–0435	18 44 41.5	–04 35 14	—	—	—	—	—
CB 179	2	19018–0525	19 01 50.4	–05 25 34	—	200	IX	1	A
CB 184	3	19116+1623	19 11 41.3	16 23 14	L709	300	X	1	A
CB 188	1	19179+1129	19 17 54.0	11 29 56	—	300	X	1	A
CB 189-2	3	19183+1123	19 18 22.9	11 23 14	L767	300	X	1	A
CB 189-3	3	19184+1118	19 18 24.4	11 18 09	—	—	—	—	—
CB 205	1	19433+2743	19 43 21.7	27 43 37	L810	2000	XI, b, d	3, 9, 10	B
CB 214	?	20018+2629	20 01 52.8	26 29 48	L814	700	XII	1, 11	A
CB 216	1	20037+2317	20 03 43.4	23 17 55	L797	700	XII	1, 11	A
CB 222	2	20328+6351	20 32 49.9	63 52 00	L1094	450	XIV	1, 12	A
CB 224	1	20355+6343	20 35 33.9	63 43 08	L1100	450	XIV	1, 12	A
CB 228	4	—	20 50 00.0	56 04 26	—	800	XIII	1, 11	A
CB 230	1	21169+6804	21 16 54.4	68 04 52	L1177	450	XIV, (XVI)	1, 12, 13	A
CB 232	1	21352+4307	21 35 14.4	43 07 05	B158	600	XVIII	3	B
CB 238	4	—	22 11 15.0	40 46 38	—	500	a		C
CB 240	1	22317+5816	22 31 45.9	58 16 26	L1192	500	a		C
CB 242	4	—	23 09 50.0	61 22 45	L1225	700	XV	1, 14	A
CB 243	1	23228+6320	23 22 52.9	63 20 04	L1246	700	XV	1, 14	A
CB 244	1	23238+7401	23 23 48.8	74 01 08	L1262	180	c, (III)	1, 15, 6, 18	B
CB 246	4	—	23 54 12.0	58 17 47	L1253	140	d, (III)	1, 16, 6, 18	B

**Table 1.** (continued)

Associations:

(I) Near side of Perseus arm; (II) “-12 km/s” clouds; (III) Lindblad ring clouds; (IV) Taurus dark cloud complex; (V) Gemini OB1 molecular clouds; (VI) Vela OB1 cloud complex; (VII) Ophiuchus dark cloud complex; (VIII) BBW101; (IX) Aquila Rift; (X) Cloud B; (XI) Vul OB1 cloud complex; (XII) Cygnus Rift; (XIII) Cyg OB7 molecular cloud complex; (XIV) Cepheus Flare molecular cloud complex; (XV) Cepheus OB3 molecular cloud complex; (XVI) NGC 7023; (XVII) Cloud “bridge” between Ophiuchus cloud and Aquila rift; (XVIII) S 126.

Methods:

(a) Average distance, see text; (b) Kinematic distance; (c) Lack of foreground stars; (d) Photometric distance.

References and Remarks:

(1) Dame et al. 1987; (2) Ungerechts & Thaddeus 1987; (3) Brand & Blitz 1993; (4) Bok & Cordwell McCarthy 1974 (5) Carpenter et al. 1995; (6) Lindblad et al. 1973; (7) Reipurth & Graham 1988; (8) Nozawa et al. 1991; (9) Neckel & Staude 1990; (10) Hilton & Lahulla 1995; (11) Dame & Thaddeus 1985; (12) Lebrun 1986; (13) Elmegreen & Elmegreen 1978; (14) Sargent 1977; (15) Kun 1997; (16) Snell 1981; (17) Yun & Clemens 1994a:  $D_{\text{kin}} = 2.1$  kpc; (18) Sandqvist et al. 1988; (19) Sandqvist & Lindroos 1976.

**Table 2.** Observational parameters

Telescope	Period	$\lambda_0$ (mm)	$\theta_b$	Chopper throw	Zenith opacity
30-m MRT	Dec. 92	1.27	12''	60''	0.4...0.6
30-m MRT	Mar. 93	1.27	12''	60''	0.3...0.5
15-m SEST	Mar. 93	1.27	23''	70''	0.2...0.5
15-m SEST	Mar. 94	1.27	23''	70''	0.2...0.3

their boundaries and 15 globules with no IRAS point source associated. Since 3 globules of our list have two IRAS point sources within their boundaries (CB 107, CB 155, and CB 189), a total number of 47 IRAS point sources was observed. Note that with the given selection criteria, our sample is strongly biased towards globules with active star formation and is, thus, not representative of the galactic population of Bok globules.

The names and coordinates of the associated IRAS point sources are given in Table 1. The coordinates are taken from the IRAS point source catalog. For globules which are not associated with IRAS point sources, the coordinates given refer to the optical centers of the globules and are taken from C&B88. In addition, we list the group membership of the globules.

### 3. Observations and data reduction

The 1.3 mm continuum survey was performed during four observing runs between December 1992 and March 1994 using the 15-m SEST telescope at La Silla, Chile (ESO N° 50.C-4032 and N° 52.C-5001) and the 30-m IRAM telescope (MRT) on Pico Veleta, Spain. At both telescopes,  $^3\text{He}$ -cooled bolometer systems developed by the Max Planck Institute for Radio Astronomy were used (Kreysa 1990; Thum et al. 1992). The equivalent bandwidth of the bolometers was  $\approx 50$  GHz centered on a frequency of 236 GHz ( $\lambda_0 = 1.27$  mm). The effective beam sizes  $\theta_b$  (HPBW) at this wavelength amount to 23'' and 12'' at the 15-m SEST and the 30-m MRT, respectively. The observational parameters are summarized in Table 2.

We followed the standard observing procedure, i.e., pointing the telescope on a nearby bright quasar by doing cross scans followed by ON-ON measurements on the source position. At the

MRT, chopping was provided by a wobbling secondary operating at 2 Hz with a beam separation of 60'' in azimuth. Beam-switching was done by nodding the telescope after 10 sec of integration by 60'' in azimuth and thus putting the object from one beam into the other. Generally, 5 ON-ON pairs with a total integration time of 100 sec formed one measurement; the number of measurements spent on one object (2 to 5) depended on the achieved signal-to-noise ratio. At the SEST, chopping was provided by a focal plane chopper operating at 6 Hz with a beam separation of 70'' in azimuth. 10 ON-ON pairs with a total integration time of 200 sec formed one measurement.

The atmospheric transmission was usually measured by skydips every two hours. Telescope pointing and focus were checked more frequently. Pointing was found to be repeatable within  $\pm 4''$  at the MRT and within  $\pm 5''$  at SEST. The planets Uranus and Neptune were used as primary calibration standards, adopting brightness temperatures of 96 K for Uranus and 92 K for Neptune (Griffin & Orton 1993). We estimate the total calibration uncertainty to be  $\approx 20\%$ . Average  $3\sigma$  detection limits were 17 mJy/12'' beam at the MRT and 39 mJy/23'' beam for SEST observations.

The raw data were first de-spiked, averaged for each ON-ON pair, and corrected for the atmospheric extinction using the approximation of a plane-parallel atmosphere. The mean value of all measurements towards one position was averaged by using weighting factors of  $\sigma_i^{-2}$  where  $\sigma_i$  are the standard deviations of each ON-ON pair.

### 4. Distances

In order to derive physical parameters from the data and to compare the properties of different objects, one has to know the distances towards the globules. There are, however, only very few globules with reliably determined distances. Even the recent compilation of distances of Lynds dark clouds by Hilton & Lahulla (1995) includes only very few globules. For their catalogue sample, C&B88 used the scale height of the galactic latitude distribution of the globules together with the assumption that the globules have the same scale height as larger molecular clouds to derive an average distance of 600 pc.

A basic problem of distance determinations is that many Bok globules are simply too small and too opaque to apply star

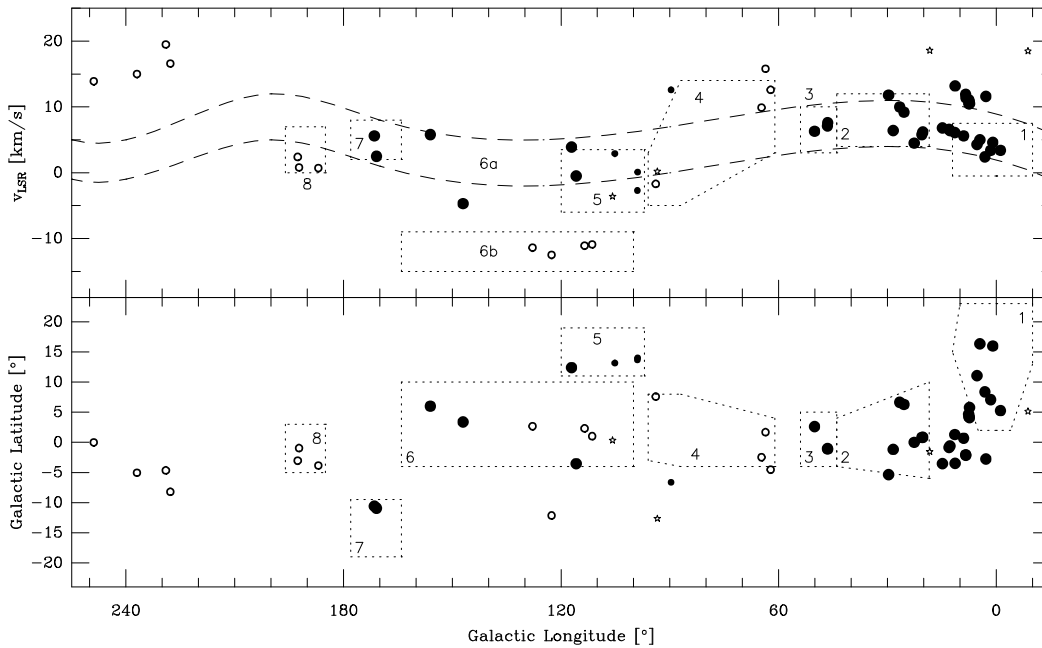


**Fig. 3.** Galactic distribution of the observed globules. Lower panel: Longitude-latitude diagram. Upper panel: Longitude-velocity diagram. Local globules which are located within 300 pc from the Sun and which are related to Gould’s Belt are marked by large filled circles. Globules at 400–600 pc are marked by small filled circles and globules at larger distances are marked by small open circles. Globules which had to be assigned to the average distance of 500 pc are indicated by asterisks. The dashed band in the upper panel marks the longitude-velocity relation of the local expanding system of dark clouds which is related to Gould’s Belt (Lindblad et al. 1973; Sandqvist et al. 1988). Some selected molecular cloud complexes are marked by rectangular dotted boxes: (1) Ophiuchus dark cloud complex (160 pc), (2) Aquila rift (200 pc), (3) Cloud B (300 pc), (4) Cygnus rift (700 pc), (5) Cepheus Flare molecular cloud complex (450 pc), (6a) Lindblad Ring - Gould’s Belt ( $\approx$  200-300 pc), (6b) “-12km/s” clouds (800 pc), (7) Taurus dark cloud (140 pc), (8) Gem OB1 cloud complex (1.5 kpc).

counts or photometric methods as distance estimators. The total absence of foreground stars towards many globules with angular diameters of  $2' - 8'$  suggests, however, that these globules cannot be further away than about 500 pc (Bok & Cordwell-McCarthy 1974). Globules which are much further away can, in general, no longer be distinguished on optical images against the stellar background. Due to this selection effect, most of the known Bok globules are assumed to be located within 1 kpc around the Sun in the local spiral arm. Here, the radial velocities ( $v_{\text{LSR}}$ ) are dominated by peculiar motions rather than by the systematic rotational velocity field of the galaxy. Therefore, the kinematic method of distance determination does, in general, not work.

Even if there is only very little known about the origin of Bok globules, they must have formed from a more extended component of the interstellar medium. One hypothesis is that Bok globules were formed from dense cores of larger molecular clouds whose diffuse gas component was blown away by stellar winds of massive stars formed from the same cloud (e.g. Reipurth 1983). Our assumption is therefore that Bok globules must be less isolated than it seems to be and that most globules are associated with larger molecular cloud complexes. This can indeed be seen very clearly, e.g., in the case of CB 68 which is located at the outermost south-eastern edge of cloud Q of a molecular cloud complex in the Ophiuchus region (Nozawa

et al. 1991, see their Fig. 8g). Such physical associations can only be revealed on large-scale CO surveys because the globules which often are located in the outer, filamentary-like regions of such molecular cloud complexes appear still isolated on optical images. Hence, we compared the locations (galactic coordinates) and the  $v_{\text{LSR}}$  (taken from the  $^{12}\text{CO}$  survey of CYH91) of the globules of our list with those of larger molecular cloud complexes taken from other galactic CO surveys (e.g. Dame et al. 1987). If a globule is located within the boundaries or the near environment of a known molecular cloud complex and also corresponds to this cloud in the velocity space ( $v_{\text{LSR}}$ ), it was assigned to this cloud complex and its known distance.

Fig. 3 shows the galactic distribution (latitude and velocity over longitude) of all globules of our sample together with the boundaries of some selected molecular cloud complexes. The distances of the globules of our sample estimated in this way, together with the associated molecular cloud structures, are listed in Table 1. In addition, we assigned a reliability class to every estimated distance. Class A means that the association is reliable and the given distance can be assumed to be accurate within 30% (e.g. CB 68). Class B means that the distance estimate is only based on the low number of foreground stars or that the distance of the associated cloud structure itself is not very accurate (e.g. the “Lindblad Ring” or kinematic distances). Those globules which could not be associated with any known molec-

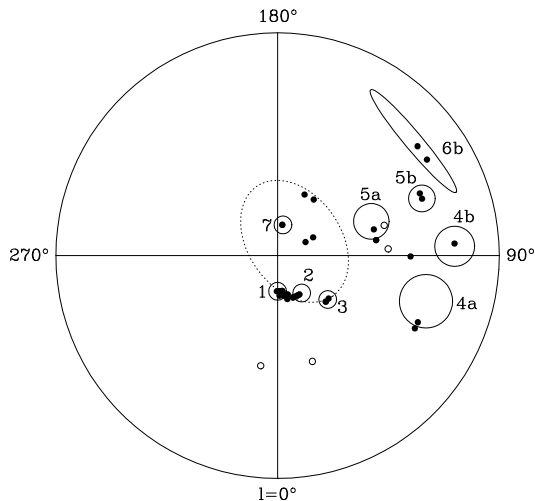


**Fig. 4.** Galactic distribution of the observed globules within 1 kpc. Longitude-distance diagram. The globules are marked by black dots. Globules which had to be assigned to the average distance of 500 pc are indicated by small open circles. Some selected molecular cloud complexes are marked by open circles or ellipses. The large, dashed ellipse in the centre marks the location of Gould's Belt. The radius of the field is 1 kpc. (1) Ophiuchus dark cloud complex, (2) Aquila rift, (3) Cloud B, (4a) Cygnus rift, (4b) Cyg OB7 cloud complex, (5a) Cep Flare molecular cloud complex, (5b) Cep OB3 cloud, (6b) "-12 km/s" clouds, (7) Taurus dark cloud.

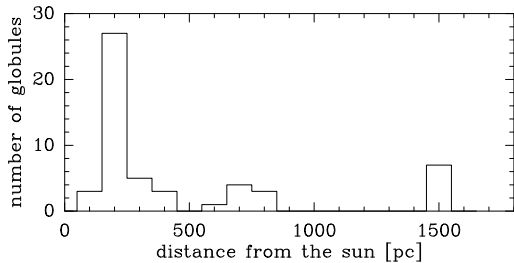


**Fig. 5.** Distance distribution of the observed globules. The width of the bins is 100 pc.

ular cloud structure (e.g. CB 69) were assigned to the reliability class C and to the average distance of 500 pc (see below).

The average distance of our entire sample is 500 pc which is only marginally smaller than the distance of 600 pc derived by C&B88. We have to mention that, due to our selection criteria (opaque globules, strong IRAS sources), the average distance of our sub-sample might be, in fact, smaller than that of the complete CB sample. Thus, we confirm the value of the average distance of the CB globules derived by C&B88 using a completely different method. However, one also has to consider that the individual globules are not randomly distributed in space.

Fig. 4 shows that most globules ( $\approx 30$ ) seem to be related to Gould's Belt and Lindblad's Feature A (the "Lindblad ring"), an expanding super-shell of early-type stars and dark clouds at an average distance of 200–300 pc (Lindblad et al. 1973; Sandqvist & Lindroos 1976). Eight other globules are related

to the "-12 km/s clouds", a string of OB associations within the local arm at a distance of 600–800 pc (Dame et al. 1987). A small number of globules (7) in the third quadrant (Gemini and Vela) is found to be at a larger distance of 1.5 kpc. This behaviour is elucidated in Fig. 5. Of the three peaks which appear in this diagram, only the innermost one which is related to Lindblad's local expanding ring is believed to be a distinct layer of matter. The two other peaks at 700 and 1500 pc are both related to the so-called "other local feature" or the "Orion arm" (see Sandqvist & Lindroos 1976), the local arm on the inner side of which the Sun and Lindblad's ring are located (e.g. Cohen et al. 1980).

It is important to note that there are remarkable differences between the average distances of the different globule groups (see Sect. 2). The average distances of the single and multiple group 1 sources (see Sect. 6.2), the group 2, 3, and 4 globules are 450, 1300, 400, 220, and 300 pc, respectively. This behaviour can be understood as a pure selection effect. Since, at large distances, only the largest, i.e., the most massive globules which naturally tend to form multiple systems (see Sect. 6.2) can be seen, the average distance of this special sub-group is larger than the one of the other globule groups. Since we selected *all* group 1 globules but *only* the most opaque group 4 globules from the CB catalogue, the difference of the average distances between these two groups is also a selection effect. As we will suggest in Sect. 6.1, the group 3 globules are already in the stage of dissipation so that only the most nearby globules could be identified from the POSS plates by C&B88 and the CB catalogue is likely to be biased towards smaller distances for this group.

The only globule which was found to be located outside the local arm but at the near side of the "Perseus" arm is CB 3. The kinematic distance of 2.5 kpc which we determined with the galactic rotation curve of Brand & Blitz (1993) is in good agreement with the value of 2.1 kpc obtained by Yun & Clemens (1994a) with the rotation curve of Clemens (1985). Due to its large distance and, consequently, its large mass it is distinguished from all other Bok globules and will be excluded from the discussion.

In this way, about 50% of the globules of our sample could be clearly assigned (reliability class A) to molecular cloud complexes of known distance. For more than 90% of the globules, we obtained reliable distance estimates (classes A and B). The high number of globules which are associated with larger molecular clouds, cloud complexes, or stellar associations shows how efficient our method of estimating distances for globules works in general. It also supports the idea that globules have formed from dense cores in larger molecular clouds and were separated from the surrounding medium only later.

## 5. Results and derived properties

Out of the 59 globules observed, 21 objects were detected above the given  $3\sigma$  limits (see Sect. 3 and Table 3). This corresponds to an overall detection rate of 35%. Out of these 21 globule cores, 18 objects are associated with IRAS point sources and 3 objects with globules of group 4. The detection rates for globules with

and without IRAS point sources are 40% and 20%, respectively. The detection rates will be discussed in more detail in Sect. 6.3.

The measured 1.3 mm flux densities per beam are compiled in Table 3 together with the r.m.s. noise, beam sizes and IRAS PSC fluxes. For non-detections, we give the  $3\sigma$  detection limits. If not indicated otherwise, the positions observed are the IRAS PSC positions listed in Table 1. For two objects (CB 3 and CB 26) which were detected on bolometer maps only, we list the peak fluxes together with the peak positions which were taken from the maps (Launhardt 1996; Stecklum et al. 1997). Their mm peak positions deviate by more than the beam size from the IRAS positions. Most of the detected sources were meanwhile mapped with a bolometer array at the IRAM MRT. In Table 3, we list the source morphology obtained from the continuum maps. The maps will be discussed in more detail in a succeeding paper (Launhardt et al. 1997b).

Table 3 also lists the bolometric luminosities  $L_{\text{bol}}$  calculated between 1 and  $1300\ \mu\text{m}$ , the 1.3 mm luminosities  $L_{1.3\text{mm}}$  as well as the total gas mass per beam derived from the 1.3 mm flux density for the sources detected at this wavelength. If a source was not detected in the lower IRAS bands, a value of one half of the upper limit was adopted for the last non-detected band to calculate the luminosity. The flux densities of all other non-detected bands were set to zero. The NIR photometry was taken from Launhardt (1996). The NIR emission (1 to  $7\ \mu\text{m}$ ) generates 0% (CB 17) to 11% (CB 6) of the bolometric luminosities of the sources, and the contribution from shorter wavelengths can be neglected. The luminosity derived this way may be very different from the bolometric luminosity if the source is not spherically symmetric (see, e.g., Men'shchikov & Henning 1997). The 1.3 mm luminosity  $L_{1.3\text{mm}}$  is calculated with a bandwidth of  $\delta\nu = 50\ \text{GHz}$ . Note that these values refer to the beam area only which is smaller than the source in most cases, whereas the contribution from the IRAS bands to the bolometric luminosities originates from the entire dense cores.

The total gas mass per beam is derived from the 1.3 mm flux density by:

$$M_{\text{g}} = \frac{S_{\nu} D^2}{\kappa_{\text{m}}(\nu) B_{\nu}(T_{\text{d}})} \left( \frac{M_{\text{g}}}{M_{\text{d}}} \right), \quad (2)$$

assuming optically thin thermal dust emission and an isothermal, uniformly distributed population of dust grains. Here,  $B_{\nu}$  denotes the Planck function,  $T_{\text{d}}$  the dust temperature,  $D$  the distance to the object,  $\kappa_{\text{m}}$  the dust opacity (mass absorption coefficient per gram dust), and  $(M_{\text{g}}/M_{\text{d}})$  the gas-to-dust mass ratio. Following Draine & Lee (1984), we assume a standard hydrogen-to-dust mass ratio of  $(M_{\text{H}}/M_{\text{d}})_{\odot} \approx 110$ . Accounting for He and metals, the total gas-to-dust mass ratio is  $(M_{\text{g}}/M_{\text{d}}) \approx 150/(Z/Z_{\odot})$ , where  $(Z/Z_{\odot})$  is the relative metallicity. Adopting  $(Z/Z_{\odot}) = 1$ , Eq.(2) can be rewritten as

$$\left( \frac{M_{\text{g}}}{M_{\odot}} \right) \approx 1.8 \cdot 10^{-14} \frac{\left( \frac{S_{\nu}}{\text{Jy}} \right) \left( \frac{\lambda}{\mu\text{m}} \right)^3 \left( \frac{D}{\text{pc}} \right)^2}{\left( \frac{\kappa_{\text{m}}(\nu)}{\text{cm}^2\text{g}^{-1}} \right)} (e^x - 1), \quad (3)$$

where  $x \approx 1.44 \cdot 10^4 / \left( \frac{\lambda}{\mu\text{m}} \frac{T}{\text{K}} \right)$ .

In order to account for the different nature of the objects assigned to different groups, we use different dust temperatures and opacities. For the group 1, 2, 3, and 4 sources we use mass-averaged dust temperatures and opacities of 25 K and  $0.8\ \text{cm}^2/\text{g}$ , 20 K and  $0.8\ \text{cm}^2/\text{g}$ , 45 K and  $2\ \text{cm}^2/\text{g}$ , and 20 K and  $0.8\ \text{cm}^2/\text{g}$ , respectively. An opacity per g of interstellar dust of  $\kappa_{\text{m}}(1.3\ \text{mm}) = 0.8\ \text{cm}^2/\text{g}$  was proposed by Ossenkopf & Henning (1994) for coagulated grains in protostellar cores of intermediate density ( $n_{\text{H}} \approx 10^5 \dots 10^6\ \text{cm}^{-3}$ ). In contrast to the group 1, 2, and 4 sources, the thermal dust emission of the group 3 sources is suggested to originate mainly from accretion disks (see Sect. 6.1) rather than from dense cores. Therefore, we adopt here a dust opacity value of  $\kappa_{\text{m}}(1.3\ \text{mm}) = 2\ \text{cm}^2/\text{g}$  (accounting for the higher coagulation grade of the dust grains in such disks; see, e.g., Beckwith et al. 1990) and a mass-averaged dust temperature of 45 K which is typical for disks around classical T Tauri stars (see, e.g., Beckwith et al. 1990 and Osterloh & Beckwith 1995). For the sources of groups 2 and 4 (candidate pre-protostellar cores), we adopt  $T_{\text{d}} = 20\ \text{K}$  which is an upper limit for isothermal cores (see, e.g., Shu et al. 1987; Mezger et al. 1988; Bontemps et al. 1995). The average dust temperature of the group 1 sources is derived from greybody fits to the FIR/sub-mm SEDs of ten of these sources (Launhardt et al. 1997a). The value of 25 K is equal to the lower boundary of the FIR colour temperature range of this group (see Sect. 2). The FIR colour temperature is assumed to overestimate the effective temperature of the bulk of the dust in the dense cores due to the different beam sizes and due to the presence of very small grains (see, e.g., discussion in Launhardt et al. 1997a).

To approximately correct the derived masses for the actual dust temperature, the mass has to be scaled with  $T_{\text{d}}(\text{adopted})/T_{\text{d}}$  for  $T_{\text{d}} > 20\ \text{K}$ . This also means that the derived masses are not very sensitive to the adopted temperature in the range between 20 and 50 K. A decrease of  $T_{\text{d}}$  from 20 to 15 K would yield, however, an increase of the mass by a factor of two which could possibly apply to the pre-protostellar cores.

There is a broad spectrum of masses ranging from 0.01 to  $30\ M_{\odot}$ /beam, with the maximum of the distribution being at  $0.4\ M_{\odot}$ /beam. The majority of the sources has bolometric luminosities between 1 and  $15\ L_{\odot}$ . There is, however, a small number of objects having higher luminosities between 40 and  $500\ L_{\odot}$  (CB 3 has  $L_{\text{bol}} = 930\ L_{\odot}$ ). The masses and luminosities will be discussed in more detail in the next Section.

## 6. Discussion

### 6.1. Correlation between mm fluxes, optical and infrared properties

The FIR colour index was introduced in Sect. 2 to classify the IRAS point sources which are associated with the star-forming globule cores or young stars, respectively. This index is a rough measure of the ‘‘effective’’ dust temperature of the dense cores including possibly embedded accretion disks. On the other hand, the 1.3 mm continuum emission is a measure of the mass of these dense cores as long as the assumption of optically thin emission

**Table 3.** Results – IRAS and 1.3 mm fluxes, luminosities, and masses

CB No.	IRAS Name	$S_{12}$ [Jy]	$S_{25}$ [Jy]	$S_{60}$ [Jy]	$S_{100}$ [Jy]	$S_{1.3\text{mm}}$ [mJy/ $\Omega_b$ ]	$\theta_b$ [']	$L_{\text{bol}}$ [ $L_{\odot}$ ]	$L_{1.3\text{mm}}$ [ $L_{\odot}/\Omega_b$ ]	$M_{\text{gas}}$ [ $M_{\odot}/\Omega_b$ ]	Remarks <sup>a)</sup>
<b>3<sup>b)</sup></b>	00259+5625	0.76	1.12	30.56	108.50	<b>436 ± 16</b>	12	9.3E+2	4.2E−2	7.2E+1	EP
<b>6</b>	00465+5028	<0.25	1.01	3.96	8.96	<b>55 ± 6</b>	12	1.2E+1	5.5E−4	9.3E−1	EP
12	01354+6447	<0.25	<0.25	0.60	7.88	< 15	12	–	–	–	
<b>17</b>	04005+5647	<0.45	<0.25	0.91	5.78	<b>37 ± 6</b>	12	8.0E−1	5.2E−5	1.2E−1	E(P)
22	–	–	–	–	–	< 48	12	–	–	–	
23	–	–	–	–	–	< 42	12	–	–	–	
<b>26<sup>c)</sup></b>	04559+5200	<0.27	<0.32	4.88	11.08	<b>160 ± 14</b>	12	3.0E+0	2.2E−4	3.8E−1	P
<b>34</b>	05440+2059	0.88	2.87	10.68	28.66	<b>99 ± 9</b>	23	1.3E+2	3.5E−3	5.9E+0	EP
39	05591+1630	4.53	9.86	7.27	10.64	< 30	23	–	–	–	
45	–	–	–	–	–	< 36	23	–	–	–	
<b>52</b>	06464−1650	0.61	0.80	9.53	38.41	<b>33 ± 8</b>	23	1.0E+2	1.2E−3	2.0E+0	EP
<b>54</b>	07020−1618	0.57	3.66	43.34	111.50	<b>520 ± 10</b>	23	4.0E+2	1.8E−2	3.1E+1	EP
<b>58-2</b>	07161−2336	<0.25	0.27	3.34	14.11	<b>39 ± 9</b>	23	4.2E+1	1.4E−3	2.3E+0	
60-1	08026−3122	1.64	2.39	19.73	67.04	< 45	23	–	–	–	
67	16482−1906	0.65	<0.36	<0.46	<10.57	< 36	23	–	–	–	
<b>68</b>	16544−1604	<0.25	1.48	19.46	33.65	<b>276 ± 9</b>	23	2.1E+0	1.1E−4	1.9E−1	EP
69-2	16595−3311	1.61	1.49	<1.44	26.75	< 33	23	–	–	–	
78	–	–	–	–	–	< 48	23	–	–	–	
80	–	–	–	–	–	< 42	23	–	–	–	
81	17193−2705	<0.72	6.19	6.73	<10.89	< 48	23	–	–	–	
82	17194−2351	6.11	2.71	<0.59	<16.85	< 39	23	–	–	–	
92	–	–	–	–	–	< 30	23	–	–	–	
95	–	–	–	–	–	< 36	23	–	–	–	
97-2	17438−2017	2.48	1.49	<0.74	<10.35	< 51	23	–	–	–	
<b>98</b>	–	–	–	–	–	<b>40 ± 10</b>	23	–	1.6E−5	3.6E−2	
107-1	17597−2754	1.66	1.30	<14.42	<268.90	< 63	23	–	–	–	
107-2	17597−2749	4.33	1.12	<15.21	<205.10	< 15	23	–	–	–	
108	18001−2023	7.28	4.15	<24.61	<203.80	< 42	23	–	–	–	
110	18032−1826	1.27	<1.03	<5.12	<87.65	< 30	23	–	–	–	
114	18093−2241	6.57	4.20	<16.79	<168.00	< 45	23	–	–	–	
116-2	18095−2246	1.83	1.34	<14.28	27.96	< 39	23	–	–	–	
125-2	18127−1803	2.70	1.86	<30.39	<226.80	< 60	23	–	–	–	
126	–	–	–	–	–	< 45	23	–	–	–	
<b>130</b>	–	–	–	–	–	<b>67 ± 15</b>	23	–	4.1E−5	9.4E−2	E(P)
131	–	–	–	–	–	< 21	23	–	–	–	
135-1	18203−2047	<0.28	<0.35	2.21	27.29	< 30	23	–	–	–	
138	18221−1055	<3.65	2.93	12.50	<219.70	< 30	23	–	–	–	
139	18225−1043	<1.29	0.76	<22.52	<367.60	< 60	23	–	–	–	
142	18272−1343	0.95	0.68	<10.18	<222.50	< 60	23	–	–	–	
143	18274−1743	3.09	0.93	<10.68	<100.70	< 51	23	–	–	–	
<b>145</b>	18296−0911	1.58	<4.03	<65.10	<267.00	<b>43 ± 9</b>	23	1.8E+1	2.7E−5	9.1E−3	
155-1	18445−0440	1.94	1.29	<23.35	59.34	< 42	23	–	–	–	
155-2	18446−0435	4.58	2.84	<10.74	<136.40	< 42	23	–	–	–	
179	19018−0525	<0.25	<0.25	0.75	7.42	< 33	23	–	–	–	
184	19116+1623	0.97	0.58	<0.98	<8.93	< 15	12	–	–	–	
<b>188</b>	19179+1129	<0.27	1.06	3.93	18.48	<b>60 ± 9</b>	12	2.5E+0	8.4E−5	1.4E−1	EP
189-2	19183+1123	0.96	0.50	<5.53	<82.50	< 60	12	–	–	–	
189-3	19184+1118	2.95	1.07	<5.45	<71.62	< 48	12	–	–	–	
<b>205</b>	19433+2743	1.07	4.91	30.13	83.97	<b>67 ± 9</b>	12	6.1E+2	4.2E−3	7.1E+0	EP
214	20018+2629	0.21	0.52	0.88	<21.58	< 21	12	–	–	–	
216	20037+2317	1.87	5.57	10.95	17.65	< 24	12	–	–	–	
222	20328+6351	<0.25	<0.25	0.53	3.97	< 39	12	–	–	–	
<b>224</b>	20355+6343	0.26	0.90	2.99	8.19	<b>41 ± 7</b>	12	3.9E+0	1.3E−4	2.2E−1	EP
228	–	–	–	–	–	< 45	12	–	–	–	
<b>230</b>	21169+6804	<0.25	0.68	11.75	33.53	<b>221 ± 5</b>	12	1.2E+1	6.9E−4	1.2E+0	EP
<b>232</b>	21352+4307	1.02	3.55	6.86	13.89	<b>20 ± 6</b>	12	1.4E+1	1.1E−4	1.9E−1	EP
238	–	–	–	–	–	< 24	12	–	–	–	
<b>240</b>	22317+5816	<0.58	0.76	6.89	22.47	<b>28 ± 6</b>	12	7.3E+0	1.1E−4	1.9E−1	EP
242	–	–	–	–	–	< 30	12	–	–	–	
<b>243</b>	23228+6320	0.26	0.74	2.06	7.98	<b>98 ± 4</b>	12	1.0E+1	7.4E−4	1.3E+0	EP
<b>244</b>	23238+7401	<0.25	0.78	9.60	15.20	<b>100 ± 9</b>	12	1.3E+0	5.0E−5	8.6E−2	EP
<b>246</b>	–	–	–	–	–	<b>33 ± 9</b>	12	–	1.0E−5	2.3E−2	E

**Table 3.** (continued)

- a) Morphology if a 1.3 mm continuum map exists: E = extended source; EP = extended source with compact component(s); P = point source.
- b) 1.3 mm peak position R.A. =  $00^{\text{h}}25^{\text{m}}56^{\text{s}}.9$  Dec. =  $56^{\circ}25'31''$ , deviates from IRAS position (Table 1).
- c) 1.3 mm peak position R.A. =  $04^{\text{h}}55^{\text{m}}54^{\text{s}}.7$  Dec. =  $52^{\circ}00'14''$ , deviates from IRAS position (Table 1).

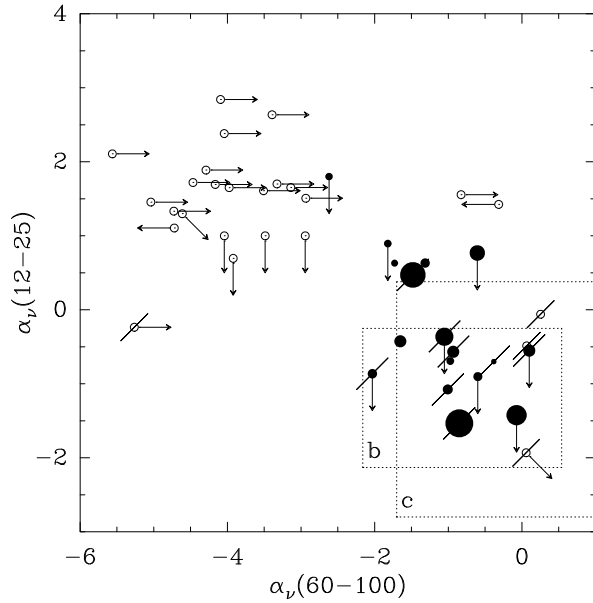


**Fig. 6.** Colour-colour diagram of all IRAS point sources of our sample which have at least one defined IRAS colour. Sources which were detected at 1.3 mm are marked by filled circles. The circle size is scaled with the measured flux density at 1.3 mm. Sources which were not detected at 1.3 mm are marked by open circles. Sources which are associated with molecular outflows are marked by diagonal lines. The arrows give the direction of the shift in the diagram if one considers that some IRAS flux density values are only upper limits. The dotted rectangular boxes mark the same object classes as in Fig. 1.

holds. Both quantities change during the star formation process. It is therefore obvious to investigate the correlation between the IRAS colours and the 1.3 mm continuum fluxes.

In Fig. 6, the mid-IR spectral index  $\alpha_{\nu}(12-25)$  and the FIR spectral index  $\alpha_{\nu}(60-100)$  (see Eq. 1) of all IRAS point sources within our sample are shown in a colour-colour diagram (comp. Fig. 1). In addition, the diagram shows which sources were detected at 1.3 mm continuum and which sources are associated with molecular outflows (Yun & Clemens 1992).

Within the sample of Bok globules associated with IRAS point sources and with two exceptions (CB 17 and CB 145), only sources with  $-2.3 < \alpha_{\nu}(60-100) < 0$  and  $-2 < \alpha_{\nu}(12-25) < 1$  (“group 1”) were detected at 1.3 mm. As it can be seen in the diagram (Fig. 6), molecular outflows are also nearly exclusively associated with this group of sources. The frequency of molecular outflows within this group is at least 65% (not all globules were searched for outflows yet). While a detectable 1.3 mm flux is indicative of dense and cold cloud cores, the presence of molecular outflows establishes the presence of embedded YSOs. The correlation of both charac-

teristics with the IRAS colours shows that star-forming cores among the globules can be clearly identified by their position in the IRAS colour-colour diagram. This can be understood if one considers that only gravitationally bound cores in an early stage of star formation are condensed and cold enough to be detected by IRAS as point sources with such low colour temperatures. This assumption is also supported by the fact that 15 out of the 16 group 1 detections (at 1.3 mm) are associated with NIR emission (nebularities or stars, Yun & Clemens 1994b; Launhardt 1996). The majority of these objects is located in the central opaque region of their parental globules which are, in general, more compact and opaque than the globules of group 3. Combined with the broad-band SED of this group (Fig. 2a), this leads to the conclusion that the globule cores of group 1 are internally heated cores being in an early stage of star formation (see discussion in Sect. 6.4).

In contrast, only one object of group 3 was detected at 1.3 mm (CB 145). This source is not marked in the colour-colour diagram (Fig. 6) because it was only detected at  $12 \mu\text{m}$  by IRAS. According to their broad-band SEDs (Fig. 2b), these objects are assumed to be pre-main sequence (PMS) stars. This assumption is also supported by the fact that 12 out of the 15 sources of this group which were observed at 1.3 mm are associated with visible or NIR stars. All sources of this group lie *outside* the boundaries of the opaque regions of the associated globules which mostly are not as compact and regular as the globules of group 1. The positional coincidence of such “warm” IRAS point sources with visible stars in the immediate vicinity of the globules together with the lack of massive cold dust shells indicates that these globules have recently formed stars which still have a small amount of circumstellar material probably concentrated in an accretion disk and which already moved out of their parental cloud cores. These globules are, therefore, very likely in the stage of dissipation which would explain their diffuse appearance. The relatively low 1.3 mm flux of CB 145 is, therefore, assumed to originate from a circumstellar accretion disc rather than from an extended envelope. The low detection rate within this group will be discussed in more detail in Sect. 6.3.

In order to emphasize the typical differences in the appearance of the globules of groups 1 and 3, we show the optical images of two typical globules CB 188 (group 1) and CB 143 (group 3) and mark the location of the IRAS sources in them (Fig. 7; comp. the SEDs in Fig. 2). Both globules are located close to the galactic plane, but CB 188 (300 pc) is at a larger distance than CB 143 (180 pc).

The second object detected at 1.3 mm which is associated with an IRAS point source and which does not belong to group 1 but to group 2 is CB 17. Out of the five objects of this group which were observed at 1.3 mm (CB 12, CB 17, 135, 179, and

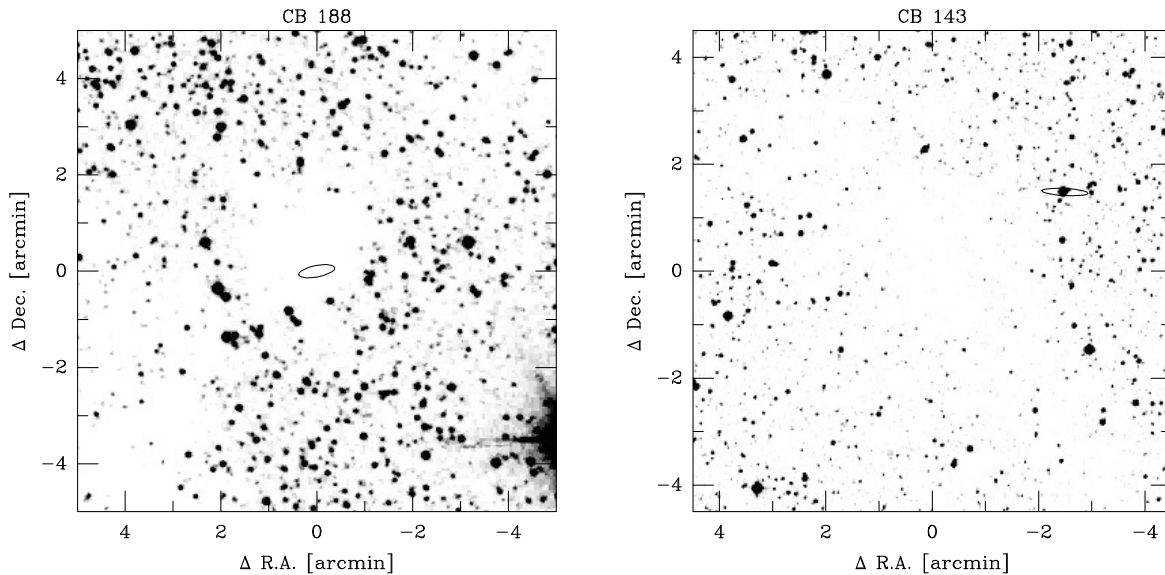


**Fig. 7.** Optical images of the globules CB 188 (group 1) and CB 143 (group 3) taken from the Digitized Sky Survey. The positions of the associated IRAS point sources are marked by their position error ellipses. The centre positions are R.A.(1950) =  $19^{\text{h}}17^{\text{m}}54^{\text{s}}.0$ , Dec.(1950) =  $11^{\circ}29'16''$  for CB 188, and R.A.(1950) =  $18^{\text{h}}27^{\text{m}}39^{\text{s}}.0$ , Dec.(1950) =  $-17^{\circ}44'45''$  for CB 143.

222), three sources (CB 12, 17, and 222) are located inside compact and opaque globules while CB 135 and CB 179 are rather diffuse clouds. While the first three objects are candidates for pre-protostellar cores (Ward-Thompson et al. 1994) or extremely young protostellar cores (“Class-I”, Boss & Yorke 1995), the latter two are probably simply cirrus clumps (comp. Fig. 1).

## 6.2. Masses and densities

The derived masses contain uncertainties of up to a factor of 2, due to the imprecisely known value of the mass opacity  $\kappa_{\text{m}}$  – see, for example, Agladze et al. (1994) and Henning & Mutschke (1997) for laboratory measurements of  $\kappa_{\text{m}}$  at long wavelengths and low temperatures and Henning et al. (1995) or Gordon (1995) for a discussion of the uncertainties in masses derived from submillimetre continuum data. It can, however, not be completely excluded that there is an unknown contribution to the mm flux from an optically thick disk. This could especially apply to the more evolved objects. In such cases, the derived mass underestimates the true mass.

Since the pre-protostellar cores as well as the protostellar cores up to “Class I” (group 4, 2, and 1 sources) are usually more extended than the beam size of the performed observations (Launhardt et al. 1997b), the derived masses of these objects which refer to the beam area only are lower limits of the total core masses. The volume densities are calculated under the assumption that the cores are spherical and match the beam size, and hence the local densities may exceed these values. In the following, we discuss the derived masses and densities for the individual object groups.

The mass spectrum of the protostellar cores of *group 1* ranges from  $0.1$  to  $30 M_{\odot}$  per beam. If one considers, however, that NIR images reveal that two of these objects are binary sources (CB 52 and 230; Launhardt et al. 1997b; Yun 1996) and that five objects show up as clusters of young stars (CB 34, 54, 58, 205, and 240; Alves & Yun 1995; Launhardt et al. 1997b; Neckel & Staude 1990), the average mass of the single objects is only  $0.5 M_{\odot}$ . The average mass of the two binary systems is  $1.6 M_{\odot}$  and the average mass of the objects which are associated with NIR clusters is  $9 M_{\odot}$  per beam. This behaviour shows that more massive cores have a greater tendency to fragment and to form multiple stellar systems than low-mass cores as it is predicted by most models. The 1.3 mm continuum emission of these objects can come from both a circumstellar accretion disk and an envelope. According to the “standard” model of protostellar envelopes, however, the 1.3 mm continuum emission of Class I and younger sources measured with an angular resolution of  $10''$  or more and at the given distances is dominated by the emission of the envelopes (Terebey et al. 1984; 1993). The average volume densities of the single and multiple cores are  $n_{\text{H}} = 8 \cdot 10^5 \text{ cm}^{-3}$  and  $n_{\text{H}} = 1 \cdot 10^5 \text{ cm}^{-3}$ , respectively. The lower volume densities of the multiple cores compared to the single cores is understandable since in these globules some “effective” position was observed rather than the center of an individual core.

For the sources of *group 2* which are probably more condensed than typical pre-protostellar cores, an average upper limit ( $3 \sigma$ ) of  $0.16 M_{\odot}$  per beam is derived with the only detected object (CB 17) having  $0.12 M_{\odot}$  per beam. The detection limit for the three sources with  $d \leq 300 \text{ pc}$  is  $0.07 M_{\odot}$  per beam. For CB 17, a beam-averaged volume density of  $n_{\text{H}} = 6 \cdot 10^5 \text{ cm}^{-3}$  is

derived which is comparable to the densities of the group 1 and 4 sources.

For the sources of *group 3*, we derive an average upper limit ( $3\sigma$ ) of  $0.013 M_{\odot}$  with the only detected object (CB 145) having  $0.009 M_{\odot}$ . These values correspond to the mass of an accretion disk around a typical classical T Tauri star ( $M_{\text{disk}} \approx 0.01 M_{\odot}$ , e.g., Beckwith et al. 1990 and Osterloh & Beckwith 1995). These objects are, in addition to the different IRAS properties, clearly distinguished from the group 1 sources by the lack of cold, massive dust envelopes.

The largest discrepancy between the derived mass per beam and the total mass must be expected for the *group 4* globules which have no IRAS point sources because their cores are the less condensed and most extended ones. The average mass per beam of the three detected objects of this group is  $0.05 M_{\odot}$  and the average column and volume densities are  $N_{\text{H}} = 2 \cdot 10^{22} \text{ cm}^{-2}$  and  $n_{\text{H}} = 5 \cdot 10^5 \text{ cm}^{-3}$ , respectively. These values are consistent with the parameters derived by Ward-Thompson et al. (1994) for a sample of pre-protostellar cores. Excluding the three most distant globules of this group, an average upper mass limit ( $3\sigma$ ) of  $0.04 M_{\odot}$  per beam is obtained for the non-detected sources.

### 6.3. Detection rates and frequency of star-forming globules

The detection rates given in Sect. 5 are not representative of the entire CB catalog because the selected sub-sample is biased towards globules with star-forming cores.

As shown in Sects. 2 and 6.1, 19 out of the 20 *group 1* globule cores which were classified as protostar candidates according to their IRAS point source properties were observed at 1.3 mm. Of these, 16 objects were detected. CB 199 (B 335) which was detected by Chandler et al. (1990) has to be added to this list. CB 3 will be excluded from the discussion due to its exceptional large distance and mass. The three non-detected sources of this group are CB 39, 60-1, and 216. CB 39 and CB 60 were also not detected in CS line emission (Sect. 6.5) and have, therefore, indeed no dense cores. The IRAS source in CB 39 is associated with the Herbig Ae/Be star HD 250550 and has an unusual  $25/60 \mu\text{m}$  flux ratio. It is, therefore, an exceptional object in this group. CB 216 which was detected in the CS line might have been missed at 1.3 mm continuum due to the uncertainty of the IRAS position which is larger than the beam size at 1.3 mm at the MRT. As mentioned in Sect. 5, two other objects (CB 3 and CB 26) were also detected in maps only because the mm positions deviate by more than the beam size from the IRAS positions. We expect, therefore, that CB 216 will also be detected in mm maps. Thus, 16 out of 17 protostar candidates (all group 1 sources except CB 3, 39, and 60) were detected which corresponds to a detection rate of 94% within this group. Since only the sources of group 1 resemble the IR and mm properties of protostellar cores of “Class 0” and “Class I”, we conclude that the relative abundance of Bok globules in the CB catalogue which currently have such protostellar cores is  $\approx 7\%$ .

Out of the 40 globules of *group 2* (16% of the entire CB catalogue), 5 globule cores were observed of which only one object (CB 17) was detected at 1.3 mm. This corresponds to

a detection rate of 20% within this group. According to their optical properties, an upper limit of the frequency of dense cores within this group of 60% can be derived (see Sect. 6.1). The low detection rate within this group is assumed to be caused by the detection limit of the observations which was in the order of the flux densities expected from these weak objects. Although some of these objects are probably more evolved than “normal” pre-protostellar cores (Ward-Thompson et al. 1994) because they have already (weak and cold) IRAS point sources, we count them here as candidates for pre-protostellar cores.

The globules of *group 3* which are assumed to be associated with PMS stars which still have a small amount of circumstellar material probably concentrated in accretion disks make 13% of all globules of the CB catalog. The actual fraction of these sources among Bok globules is, however, assumed to be higher because of the selection effect mentioned in Sect. 4. There is only one out of 15 sources of this group detected at 1.3 mm (detection rate 7%). The low detection rate – compared to mm continuum surveys of young low-mass stars (e.g., Henning et al. 1993; André & Montmerle 1994; Osterloh & Beckwith 1995) – can come from the lower effective sensitivity of our measurements. Scaling the globule sources to the distance of Taurus, our average  $3\sigma$  detection limit is higher than the mean mm flux density measured from classical T Tauri stars in the Taurus-Auriga region. The relative abundance of Bok globules which are associated with such stars can, therefore, be estimated to be between 15 and 30%. There might be, however, an unknown number of globules which are associated with PMS stars which have no or much less massive disks (e.g. wTTS).

Out of the 139 *group 4* globules which have no IRAS point sources (56% of the entire CB catalog), 15 globules were observed at 1.3 mm of which 3 objects were detected. This corresponds to a detection rate of 20% within this group which compares to the detection rate of 25% for  $\text{NH}_3$  (Sect. 6.5). These three objects are good candidates for pre-protostellar cores. Due to the imprecisely known positions of the assumed dense cores, the actual frequency of pre-protostellar cores within this group might, however, be higher than our measurements suggest. We assume here an upper limit of 50% as an order-of-magnitude estimate. On the other hand, dense and opaque globules were preferred by our selection criteria so that the relative abundance of pre-protostellar cores among all group 4 globules is probably lower than among our selected subsample. Together with the group 2 sources which should appear as “starless” cores at large distances because their IRAS point sources are very weak, the lower and upper limits of the relative abundance of Bok globules which currently have pre-protostellar cores can be estimated to be 15% and 35%, respectively.

Summarizing this discussion and considering the selection effects, the following numbers are obtained: The percentages of globules which presently contain pre-protostellar cores and protostellar cores (Classes 0 and I) are 15 – 35% and 5 – 7%, respectively. Between 15 and 30% of all CB globules formed recently stars which still have a small amount of circumstellar material and which are still located in the immediate vicinity of their parental globules. A fraction of 30 to 65% of all globules

either never forms solar-like stars, or formed stars long ago, or probably forms stars of much lower mass (or brown dwarfs) which cannot be detected with the applied methods.

On the basis of these relative frequencies, simple order-of-magnitude estimates of the lifetimes of the different evolutionary phases can be obtained. Assuming an average stellar mass of  $0.5 M_{\odot}$  and an accretion rate of  $2 \cdot 10^{-6} M_{\odot} \text{ yr}^{-1}$  (see Sect. 6.4), the accretion time which is set equal to the lifetime of the protostellar cores, is  $\approx 2.5 \cdot 10^5$  years (comp., e.g., Wilking et al. 1989). According to their relative abundance, the lifetime of the pre-protostellar cores must then be between  $0.6$  and  $1.5 \cdot 10^6$  years which is consistent with the lifetime of  $\approx 10^6$  years derived by Ward-Thompson et al. (1994) and with typical ambipolar diffusion time scales of small cloud cores (e.g. Mouschovias 1976; Shu 1992; Fiedler & Mouschovias 1993).

For the lifetime of the young stars (with strong IR excess) in the immediate vicinity of the globules (group 3), we derive  $0.5 - 1 \cdot 10^6$  years which is shorter than the typical lifetime of classical T Tauri stars, i.e., a few times  $10^6$  years (e.g. Cohen & Kuhl 1979). We suggest, therefore, that many of the group 4 globules which do not contain pre-protostellar cores, formed already stars one to a few times  $10^6$  years ago and are still associated with T Tauri stars which moved further away from the globules or whose accretion disks are already dissipated (e.g., isolated weak-line T Tauri stars). Assuming that all globules form stars at some time of their evolution, an upper limit of  $\approx 5 \cdot 10^6$  years can be derived for the average total lifetime of Bok globules after they were separated from larger molecular clouds and before they dissipate. Since this total lifetime is not much longer than the ambipolar diffusion time but is comparable or even shorter than the lifetime of the PMS phase of solar like stars, it can be expected that the majority of the PMS stars formed by globules has already “lost” their parental globules.

With these numbers, we are also able to derive the total number of T Tauri stars which are formed by Bok globules. Since the Bok globules are only loosely associated with larger molecular clouds and are not directly related to star-forming regions, it is obvious that these stars will be observed as isolated T Tauri stars (e.g. de la Reza et al. 1989). If we assume that the CB catalogue is complete for clouds inside a radius of 500 pc around the Sun (average distance) for declinations north of  $-30^\circ$  (67% of the galactic plane), the total number of Bok globules within this volume can be estimated to be  $\approx 370$ . The upper and lower limits of this number are assumed to deviate by a factor of 2 (see the discussion in CYH91). Assuming a scale height of the galactic disk (molecular clouds and young stars) of 120 pc ( $\Delta Z_{\text{FWHM}}$ ; Clemens et al. 1988), the volume density of globules amounts to  $370 / (\pi \times 120 \times 500^2) \approx 4 \cdot 10^{-6} \text{ pc}^{-3}$ . Counting only the globules within 300 pc, this number increases by a factor of 1.5 only which shows that the assumption of completeness is nearly fulfilled. Assuming further that 5% of the globules currently contain protostellar cores which form each one to two stars within  $\approx 2.5 \cdot 10^5$  years, and that the total lifetime of such a T Tauri star is  $\approx 10^7$  years (e.g., Appenzeller & Mundt 1989), the average volume density of isolated T Tauri stars formed by Bok globules amounts to  $1.5 \times 4 \cdot 10^{-6} \times 0.05 \times 10^7 / 2.5 \cdot 10^5 \approx 1 \cdot 10^{-5} \text{ pc}^{-3}$ .

Although the assumptions of a homogeneous distribution of globules (see Sect. 4) and of a constant star formation rate (e.g., Palla & Galli 1997) do certainly not hold very well, the above calculations give an order-of-magnitude estimate for the expected number of observable isolated T Tauri stars formed by Bok globules. The actual number of such stars is not known yet. There are, however, several studies related to this topic under work.

#### 6.4. Mass-luminosity ratio and evolutionary stage

In this paragraph, only the sources of group 1 and 2 which were detected at 1.3 mm will be discussed. The mass and the luminosity of a protostellar system are two important parameters which characterize its evolutionary stage. For the following, we assume that the total mass  $M_{\text{tot}}$  of the protostar-envelope system remains constant and that this mass will be completely accreted onto the star with a constant mass accretion rate (see, e.g., Stahler et al. 1980). This assumption is definitely not true for the formation of high-mass stars, but may well be used for low-mass stars. While there is no direct measure of the mass of a deeply embedded (proto-)star, the mass of the circumstellar envelope  $M_{\text{cs}}$  can be measured by its optically thin thermal dust emission at mm wavelengths. For this reason, we use the circumstellar mass  $M_{\text{cs}} = M_{\text{tot}} - M_*$  to characterize the observed systems. The luminosity of a low-to-intermediate-mass protostar during its main accretion phase mainly originates from the accretion shock on its surface. This accretion luminosity is given by  $L_{\text{acc}} = GM_* \dot{M} / R_*(M_*)$ , where  $M_*$  is the mass of the central star,  $\dot{M}$  is the mass accretion rate, and  $R_*$  is the stellar radius. It is, therefore, a measure of the stellar mass. The contribution of the stellar interior  $L_{\text{int}}$  to the total luminosity at this stage is about 10–20% for  $M_* \leq 2 M_{\odot}$  (Fletcher & Stahler 1994). The total luminosity of the protostellar system is then given by  $L_{\text{tot}} = L_{\text{acc}} + L_{\text{int}}$ . When most of the mass of the envelope is accreted onto the star, the envelope becomes optically thin and the star becomes visible and appears on the stellar “birthline” (the “upper” envelope for young stars in the H-R diagram, Stahler 1988). The total luminosity of the star ( $M_* \leq 2 M_{\odot}$ ) is now given by  $\approx L_{\text{int}}$  and amounts to only 10–25% of its former accretion luminosity.

Fig. 8 shows a mass-luminosity diagram for protostars and their envelopes. In the diagram, the mass-luminosity relation for accreting protostars is marked by dashed lines. To calculate the protostellar luminosity  $L_{\text{tot}} = L_{\text{acc}} + L_{\text{int}}$  as a function of the central stellar mass, we used the mass-radius relation for accreting protostars given by Stahler (1988) and Palla & Stahler (1990). For the mass accretion rate, a lower limit of  $2 \cdot 10^{-6} M_{\odot} \text{ yr}^{-1}$  (corresponding to an isothermal sound speed of  $c_{\text{th}} = 0.2 \text{ km s}^{-1}$  at  $T_{\text{kin}} = 10 \text{ K}$  – lower curve) and an upper limit of  $6 \cdot 10^{-6} M_{\odot} \text{ yr}^{-1}$  (considering turbulent contributions,  $c_{\text{eff}} = 0.3 \text{ km s}^{-1}$ , derived from the mean  $\text{C}^{18}\text{O}$  linewidth of  $0.5 \text{ km/s}$ , Launhardt 1996 – upper curve) were used. The interior luminosity  $L_{\text{int}}$  was taken to be equal to the birthline luminosity of a star of mass  $M_*$  and appropriate protostellar radius (see Fletcher & Stahler 1994 for a compilation of birthline lu-

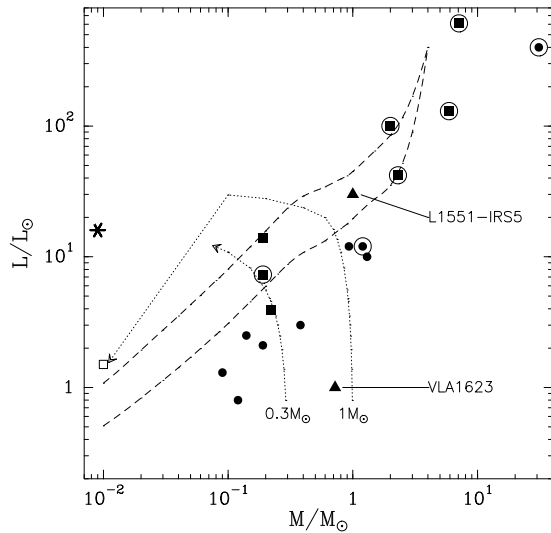


**Fig. 8.** Mass-luminosity diagram. The dashed curves indicate the theoretical mass-luminosity relation for accreting protostars using constant mass accretion rates of  $2 \cdot 10^{-6} M_{\odot} \text{ yr}^{-1}$  (lower curve) and  $6 \cdot 10^{-6} M_{\odot} \text{ yr}^{-1}$  (upper curve). Globule cores detected at 1.3 mm are marked as filled circles or squares if they are associated with visible stars. Multiple objects are, in addition, marked as large open circles. CB 145 (group 3) is marked by an asterisk. The objects are represented by their bolometric luminosity and circumstellar mass as derived from the ON-ON measurements (Table 3). The dotted curves show the evolutionary tracks of two protostellar systems of  $0.3 M_{\odot}$  and  $1 M_{\odot}$ . The open square marks the location of a typical TTS (see text). For comparison, VLA1623 and L1551-IRS5 are shown as triangles (integrated fluxes and bolometric luminosities taken from André et al. 1993). Note that the abscissa stands for the stellar mass (dashed curves) as well as for the circumstellar mass (all other symbols)!

minositities and radii). Note that all other symbols and curves in the diagram represent circumstellar masses  $M_{\text{cs}}$  and not  $M_{*}$ .

Also marked in Fig. 8 are the evolutionary tracks of two protostellar systems of  $0.3 M_{\odot}$  and  $1 M_{\odot}$  represented by their total luminosity and their *circumstellar* mass which is decreasing during the evolution. The same assumptions and parameters as discussed above were used to calculate the protostellar radius and total luminosity as a function of the protostellar mass which is growing with a constant rate. Since it is still unclear how the mass accretion rate evolves in the very late accretion phase, the exact course of the upper left parts of the tracks remains somewhat uncertain. The open square marks the location of a typical  $1 M_{\odot}$  classical T Tauri star in the diagram ( $M_{\text{disk}} = 0.01 M_{\odot}$ ). Where these evolutionary tracks cross the mass-luminosity curve of accreting protostars (dashed lines), the mass of the central protostar and of the envelope are equal. Hence, the lower right part of the tracks represent  $M_{*} < M_{\text{cs}}$  (“Class 0” protostars, André et al. 1993), while for the upper left parts  $M_{*} > M_{\text{cs}}$ .

The observed globule cores are marked in the diagram by their bolometric luminosities and by their circumstellar masses. Note, that the derived masses refer to the beam area only and

are, therefore, lower limits of the total circumstellar masses. The assumption of spherical symmetry (isotropic emission) is assumed to be fulfilled for the deeply embedded sources without optical or NIR counterparts. For the sources which already have optical or NIR counterparts it is probably not fulfilled and the bolometric luminosity can deviate from the derived value.

From Fig. 8 it can be seen that the majority of the globule cores detected at 1.3 mm has masses between  $0.2$  and  $1 M_{\odot}$ . Objects with higher masses are mostly multiple systems. It can also be seen that the majority of the globule cores has  $M_{\text{cs}}/L$ -ratios which suggest that the circumstellar masses are considerably higher than the masses of the embedded protostars. We conclude, therefore, that these core masses are of the same order as the masses of the stars which will finally be formed in these globules. In fact, the most massive star observed in a Bok globule so far is the Herbig Ae/Be star HD 250550 in CB 39 with  $M_{*} = 4.8 M_{\odot}$  (Hillenbrand et al. 1992). Those globule cores which have lower  $M_{\text{cs}}/L$ -ratios are, indeed, already associated with visible stars (Vis. or J-band) and are, thus, more evolved. The fact that nearly all of the observed sources lie below the theoretical mass-luminosity curve of accreting protostars and fulfill, thus, one important criterion of Class 0 protostars, favours the lower value of the mass accretion rate (lower curve,  $\dot{M} = 2 \cdot 10^{-6} M_{\odot} \text{ yr}^{-1}$ ).

Although we cannot exactly distinguish Class 0 and Class I protostars in this diagram due to the uncertainties of the models and the uncertainties of the circumstellar masses derived from such ON-ON measurements, we can conclude that the majority of the group 1 sources which were detected at 1.3 mm, are protostellar cores of Class 0 or I. A more detailed discussion of this topic will be undertaken in a succeeding paper (Launhardt et al. 1997b) on the basis of NIR and mm continuum maps.

### 6.5. Correlation between the mm continuum fluxes and molecular line emission

The IRAS point source fluxes and the 1.3 mm dust continuum emission were used to derive the properties and the evolutionary stage of the globule cores or the young stars which were recently formed in the globules, respectively. If the subdivision of the globule sample into four groups introduced in Sect. 2 really characterizes an evolutionary sequence, one would expect to see systematic differences between these groups in the molecular line emission too. No distance effects will be considered here.

The  $^{12}\text{CO}$  line emission (low rotational transitions) provides information about the average kinetic temperature and the global gas dynamics of the entire globules, especially if it is measured with a large aperture. We used the CO survey of CYH91 and found no systematic differences between the average line temperatures of the globule groups. There are, however, systematic differences in the sense that the mean CO line width (FWHM) of the group 1 sources is much larger (2.4 km/s) than that of the group 2 and 3 sources (1.3 km/s) which is again larger than that of the group 4 sources (1.1 km/s). Although the line broadening can have many reasons (e.g., turbulence, outflows, infall, rotation) which do not necessarily have something to do with star

formation activity, it indicates that the globules which we found to harbour dense cores being in the most active stage of the star formation (group 1) process have, indeed, a much more complex gas dynamic than all other globules. This is, of course, not surprising since most of these sources have molecular outflows (Yun & Clemens 1992).

In contrast to  $^{12}\text{CO}$ , the isotopic  $\text{C}^{18}\text{O}(2-1)$  line remains optically thin even towards the dense cores and provides, therefore, a measure of the gas column density. We compiled the integrated line intensities  $\int T_{\text{mb}} dv$  from Wang et al. (1995), Launhardt (1996), and Lemme et al. (1996) and found that the group 1 sources have the highest beam-averaged column densities (see Fig. 9). Regarding only globules nearer than 500 pc, one finds no systematic difference between the average globule diameters of the groups, but the  $\int T_{\text{mb}} dv$  value of group 1 would be still as high as 1.5 K km/s. This column density enhancement points, therefore, really to the presence of dense gas cores.

The presence or absence of dense cores which are a prerequisite of star formation can be better tested by using molecular line transitions which require high densities to be excited. We evaluated the ammonia survey (HPBW  $40''$ ) of 237 CB globules by Lemme et al. (1996) and found detection rates of 75% for group 1 sources, 42% for group 2, 21% for group 3 and 25% for group 4. Of the sources detected at 1.3 mm continuum, only CB 6, 54, 240 (group 1), as well as CB 145 (group 3) were not detected in  $\text{NH}_3$  – all others were detected. These detection rates indicate again that the incidence of dense cores is the highest within group 1, followed by the groups 2, 4, and 3. Within the subsample of which Lemme et al. (1996) derived kinetic gas temperatures, there are no systematic differences between the groups (average  $T_{\text{kin}} = 10.5$  K for groups 1, 2, and 3) with the exception that the group 4 globules (“star-less cores”) are, on average, colder by 1 K.

A better tracer for dense gas is the  $\text{CS}(2-1)$  line ( $n_{\text{crit}} \approx 6 \cdot 10^5 \text{ cm}^{-3}$ ). Using the CS survey of Wang et al. (1997), we found a high correlation (73%) between the detection rates at 1.3 mm continuum and the  $\text{CS}(2-1)$  line emission. Out of 33 globules, 18 objects were detected in both surveys, 6 objects were detected in neither survey, 7 objects were detected only in CS, and 2 objects were detected only at 1.3 mm continuum.

Fig. 9 shows the correlation between the integrated  $\text{C}^{18}\text{O}$  line intensity (column density tracer) and the  $\text{CS}(2-1)$  line peak temperature (tracer of dense cores) for the different globule groups. Group 2 and 4 are subdivided into two subgroups each here. We distinguished within the group 2 between those sources which are located inside of compact and opaque globules (CB 12, 17, and 222; “group 2a”) and the more diffuse globules (“group 2b”). Within the group 4, we distinguished between those cores which were detected at 1.3 mm (CB 98, 130, and 246; “group 4a”) and those which were not detected (“group 4b”). The diagram reveals very clearly that the sources of groups 1, 2a, and 4a have dense gas cores while all other globules do not have such cores. Among the group 3 sources which were proposed to be young stars recently formed in the associated globules, there are only a few globules which have moderately dense cores. These are probably remnants of the

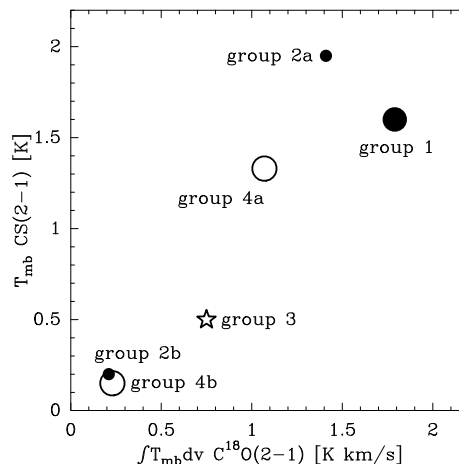


**Fig. 9.** Group-averaged CS line peak temperatures versus integrated  $\text{C}^{18}\text{O}$  line intensities. The CS line temperatures are taken from Wang et al. (1997) and the CO line intensities are taken from Wang et al. (1995), Launhardt (1996), and Lemme et al. (1996). See Sect. 2 and Table 1 for the classification of the groups. Group 2 and 4 sources are subdivided into two subgroups each here (see text).

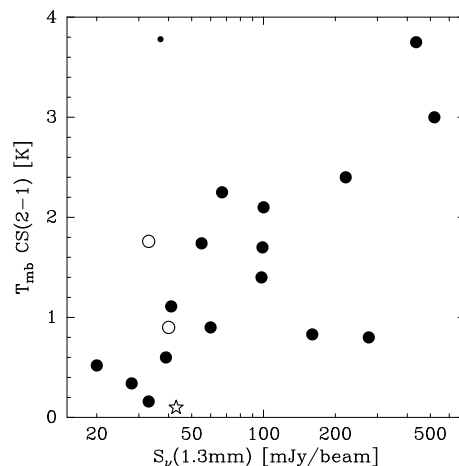


**Fig. 10.**  $\text{CS}(2-1)$  line peak temperature versus 1.3 mm flux density for all globule cores which were detected in both tracers. The CS line temperatures are taken from Wang et al. (1997). Group 1 sources are marked by large dots, group 2 (CB 17) by small dots, group 3 (CB 145) by asterisks, and group 4 (CB 98, 246) by empty circles.

cores from which these stars were recently formed. Hence, this diagram shows that the globule groups introduced in Sect. 2 and discussed in Sects. 6.1 and 6.3 are, indeed, distinguished by the incidence and properties of their dense cores.

For the sources which were detected in both the 1.3 mm dust emission and the  $\text{CS}(2-1)$  line, Fig. 10 shows a clear correlation between the continuum flux densities and the CS line peak temperatures. Three objects deviate from this correlation. The high CS line temperature and the low continuum flux of CB 17 indicate that this core has a higher average density than the group 4 sources but is not yet as strongly centrally condensed

as the group 1 sources. This is consistent with the assumption that CB 17 is presently in a transition stage between the pre-protostellar (quasi-static) phase and the protostellar (main accretion) phase. The other two exceptions which have high continuum fluxes but low CS line peak temperatures are CB 26 and 68. These three objects will be discussed in more detail in forthcoming papers (Stecklum et al. 1997; Launhardt et al. 1997b). Of the three group 1 objects which were not detected at 1.3 mm continuum, only CB 216 was detected in the CS line.

Although no distance effects nor beam sizes were considered here, this correlation shows that the 1.3 mm dust continuum emission and the CS line emission are equivalent tracers in order to detect dense, star-forming molecular cloud cores. One has to keep in mind, however, that the CS(2–1) line is usually optically thick towards such dense cores and that the CS molecule can partially freeze out from the gas phase in cold cores of high column density. Therefore, the internal structure and physical properties of these cores such as, e.g., the mass and column density, can be much more reliably derived from the 1.3 mm dust continuum emission which remains optically thin up to column densities of  $N_{\text{H}} \approx 10^{25} \text{ cm}^{-2}$  (see also the discussion in Launhardt et al. 1996).

## 7. Summary and conclusions

In search for dense, star-forming cores we surveyed 59 Bok globules for their 1.3 mm dust continuum emission using  $^3\text{He}$ -cooled single-channel bolometers with the IRAM 30 m and SEST 15 m telescopes. The globules were selected from the catalogue of C&B88 mainly according to the colours of their embedded IRAS point sources. Our sample also included 15 globules without IRAS point sources which were selected according to their optical appearance, i.e., high opacity. With effective beam sizes (HPBW) of  $12''$  and  $23''$  and average  $3\sigma$  detection limits of 17 and 39 mJy per beam, respectively, we detected 21 of the 59 objects observed.

For the first time, individual distances for most of these globules were derived with a method which associates the globules with larger molecular cloud complexes. With this method, reliable distance estimates for 90% of the globules were obtained. While we could confirm the average distance of the entire CB sample derived by C&B88 from the galactic latitude distribution width (600 pc against our value of 500 pc), we found that more than 50% of the selected globules are located in a discrete layer at 200–300 pc which is associated with Gould’s Belt and Lindblad’s Ring, an expanding super-shell of early-type stars and dark clouds. Due to selection effects, the sample is, naturally, biased towards such nearby clouds. With the exception of CB 3, which is located in the Perseus arm, all other globules are located in the local “Orion arm” at distances between 450 and 800 pc, and at  $\approx 1.5$  kpc (Gemini and Vela only).

We showed that an IRAS colour-colour diagram can serve as a powerful tool in distinguishing groups of objects which are in different stages of star formation. While other indicators of evolutionary stage, such as  $\alpha(12-25)$  (e.g. Yun & Clemens 1995) or  $L_{\text{submm}}/L_{\text{bol}}$  (André et al. 1993) can only be applied to

certain object groups (which have either MIR or submm emission), our method considers the complete MIR to FIR SEDs and can, therefore, be applied to a much more widespread sample.

Globules which currently form stars can be well distinguished from all other globules in such an IRAS point source colour-colour diagram. It was found that the mm dust continuum emission is well correlated with the colours of the embedded IRAS point sources as well as with the presence of molecular outflows. Comparing the optical, infrared, and mm properties, four distinct groups of globules which are currently in different evolutionary phases could be well-defined. From the detection rates and the relative frequencies of the different object groups, relative frequencies and lifetimes of the different evolutionary stages were derived. The following globule groups form an evolutionary sequence:

- Of the 15 globules without IRAS point sources (“group 4”) observed, three objects (CB 98, 130, and 246) were detected at 1.3 mm which are good candidates for pre-protostellar cores. Furthermore, a number of globules with extremely cold and weak IRAS point sources (group 2; e.g., CB 17) were classified as candidates for pre-protostellar cores although they are probably more evolved and are in a transition phase between quasi-static cores and Class 0 protostars. The relative frequency of globules with pre-protostellar cores is estimated to be between 15 and 35%. The lifetime of the pre-protostellar phase is derived to be  $0.6 - 1.5 \cdot 10^6$  years.
- The relative frequency of globules which currently contain protostellar cores of Class 0 and I (group 1) is derived to be 5–7%. The globules identified to be in this stage are CB 6, 26, 34, 52, 54, 58, 68, 188, 199, 205, 224, 230, 232, 240, 243, and 244. One further candidate is CB 216 which was not detected in this survey. Objects which resemble similar IR properties but are probably of different nature are CB 3 (massive object at a large distance), CB 39 (Herbig Ae/Be star HD 250550, no mm emission), and CB 60 (no mm continuum emission, no dense gas core). Assuming an average final stellar mass of  $0.5 M_{\odot}$  and a mass accretion rate of  $2 \cdot 10^{-6} M_{\odot} \text{ yr}^{-1}$ , the lifetime of the protostellar cores is derived to be  $\approx 2.5 \cdot 10^5$  years.
- A fraction of 13% of the CB globules which has no dense cores was found to have young stars in their immediate environment which still have a small amount of relatively warm circumstellar material probably concentrated in accretion disks (group 3). An average upper limit of the circumstellar mass of  $0.013 M_{\odot}$  is derived with the only detected object (CB 145) having  $0.009 M_{\odot}$ . These objects are candidates for classical T Tauri stars. Considering selection effects, the fraction of Bok globules which are associated with such stars is estimated to be 15–30%.
- A remaining fraction of 35 to 65% of globules could not be identified in this scheme. The majority of these globules is, however, assumed to have formed stars more than  $10^6$  years ago and to be still associated with, e.g., isolated weak-line T Tauri stars.

This classification is well-confirmed by observations of molecular lines such as, e.g.,  $C^{18}O(2-1)$  and  $CS(2-1)$ . Especially, the  $CS(2-1)$  line is shown to be an equivalent tracer of dense, star-forming molecular cloud cores although the internal structure and physical properties of these cores can be better derived from the optically thin 1.3 mm continuum emission.

The following general conclusions about star formation in Bok globules can be drawn from the study presented here:

1. Bok globules are not really isolated objects but are mostly loosely associated with larger molecular cloud complexes from which they were originally formed.
2. Most Bok globules form stars at some time of their evolution. Only the least massive globules which are assumed to dissipate fast, seem never to form stars.
3. The typical mass of a star formed in a Bok globule is derived to be between 0.2 and  $2 M_{\odot}$  with a mean value of  $\approx 0.5 M_{\odot}$ . More massive globule cores tend to form multiple stars rather than more massive stars.
4. Assuming an average globule mass of  $10 M_{\odot}$  (e.g., CYH91) and an average number of one to two stars formed from a globule, a typical globule transforms  $\approx 5 - 10\%$  of its total mass into stars. The remaining mass probably dissipates later.
5. Assuming that all of the observed globules form stars at some time of their evolution, an upper limit of  $\approx 5 \cdot 10^6$  years can be derived for the average total lifetime of Bok globules after they were separated from larger molecular clouds and before they dissipate.
6. The lifetime of the globules is shorter than the lifetime of the PMS phase of the stars they form. Therefore, many of the observed isolated T Tauri stars are suggested to be formed by Bok globules. The average volume density of such PMS stars formed by globules is derived to be  $\approx 10^{-5} \text{ pc}^{-3}$ . Future studies have to show whether this is the main mechanism of forming such isolated stars or not.

*Acknowledgements.* RL acknowledges support through the Verbundforschung Astronomie/Astrophysik contract No. 50 OR 9414 9.

## References

- Agladze N.I., Sievers A.J., Jones S.A., Burlitch J.M., Beckwith S.V.W., 1994, *Nature* 372, 243
- Alves J.F., Yun J.L., 1995, *ApJ* 438, L107
- André P., Ward-Thompson D., Barsony M., 1993, *ApJ* 406, 122
- André P., Montmerle T., 1994, *ApJ* 420, 837
- Appenzeller I., Mundt R., 1989, *A&AR* 1, 291
- Beckwith S.V.W., Sargent A.I., Chini R., Güsten R., 1990, *AJ* 99, 924
- Blake G.A., van Dishoeck E.F., Jansen D.J., Groesbeck T.D., Mundy L.G., 1994, *ApJ* 428, 680
- Bok B.J., 1977, *PASP* 89, 597
- Bok B.J., Reilly E.F., 1947, *ApJ* 105, 255
- Bok, B.J., Cordwell McCarthy C.S., 1974, *AJ* 79, 42
- Bontemps S., André P., Ward-Thompson D., 1995, *A&A* 297, 98
- Bourke T.L., Garay G., Lehtinen K.K., Köhnenkamp I., Launhardt R., Nyman L.-Å., May J., Robinson G., Hyland A.R., 1997, *ApJ* 476, 781
- Boss A.P., Yorke H.W., 1995, *ApJ* 439, L55
- Brand J., Blitz L., 1993, *A&A* 275, 67
- Carpenter J.M., Snell R.L., Schloerb F.P., 1995, *ApJ* 445, 246
- Clemens D.P., 1985, *ApJ* 295, 422
- Clemens D.P., Barvainis R., 1988, *ApJS* 68, 257 (C&B88)
- Clemens D.P., Sanders D.B., Scoville N.Z., 1988, *ApJ* 327, 139
- Clemens D.P., Yun J.L., Heyer M., 1991, *ApJS* 75, 877 (CYH91)
- Chandler C.J., Gear W.K., Sandell G., Hayashi S., Duncan W.D., Griffin M.J., Hazell A.S., 1990, *MNRAS* 243 330
- Cohen M., Kuhl L.V., 1979, *ApJ* 227, L105
- Cohen R.S., Cong H., Dame T.M., Thaddeus P., 1980, *ApJ* 239, L53
- Dame T.M., Thaddeus P., 1985, *ApJ* 297, 751
- Dame T.M., Ungerechts H., Cohen R.S., De Geuss E.J., Grenier I.A., May J., Murphy D.C., Nyman L.-Å., Thaddeus P., 1987, *ApJ* 322, 706
- de la Reza R., Torres C.A.O., Quast G., Castilho B.V., Vieira G.L., 1989, *ApJ* 343, L61
- Dickman R.L., Clemens D.P., 1983, *ApJ* 271, 143
- Draine B.T., Lee H.M., 1984, *ApJ* 285, 89
- Elmegreen D.M., Elmegreen B.G., 1978, *ApJ* 220, 510
- Emerson J.P., 1987, IRAS and star formation in dark clouds. In: Peimbert M., Jugaku, K.J. (eds.) *Star Forming Regions*. Reidel, Dordrecht, p.19
- Feitzinger J.V., Stuewe J.A., 1984, *A&AS* 58, 365
- Fiedler R.A., Mouschovias T.C., 1993, *ApJ* 415, 680
- Fletcher A.B., Stahler S.W., 1994, *ApJ* 435, 313
- Gee G., Griffin M.J., Cunningham C.T., Emerson J.P., Ade P.A.R., Caroff L.J., 1985, *MNRAS* 215, 15
- Gordon M. A., 1995, *A&A* , 301, 853
- Griffin M.J., Orton G.S., 1993, *Icarus* 105, 537
- Hartley, M., Manchester R.N., Smith R.M., Tritton S.B., Goss W.M., 1986, *A&AS* 63, 27
- Henning Th., Pfau W., Zinnecker H., Prusti T., 1993, *A&A* 276, 129
- Henning Th., Michel B., Stognienko R., 1995, *Planet. Space Sci.* 43, 1333
- Henning Th., Mutschke H., 1997, *A&A* (submitted)
- Henning Th., Launhardt R., 1997, *A&A* (submitted)
- Hillenbrand L.A., Strom S.E., Vrba F.J., Keene J., 1992, *ApJ* 397, 613
- Hilton J., Lahulla J.F., 1995, *A&AS* 113, 325
- Keene J., Davidson J.A., Harper D.A., Hildebrand R.H., Jaffe D.T., Loewenstein R.F., Low, F.J., Pernic R., 1983, *ApJ* 274, L43
- Kreysa, E., 1990, Sub-mm direct photometry with large telescopes. In: ESA, *From Ground-Based to Space-Borne Sub-mm Astronomy*. p.265
- Kun M., 1997, in preparation
- Lada C., 1987, Star formation - From OB associations to protostars. In: Peimbert M., Jugaku, K.J. (eds.) *Star Forming Regions*. Reidel, Dordrecht, p.1
- Ladd E.F., Lada E.A., Myers P.C., 1993, *ApJ* 410, 168
- Launhardt R. 1996, Star formation in Bok globules. PhD Thesis, University of Jena
- Launhardt R., Henning Th., 1994, Star-forming cores in Bok globules: A 1.3 mm continuum survey. In: Clemens D.P., Barvainis R. (eds.) *Clouds, cores, and low-mass stars*. ASP Conf. Ser. 65, p.224
- Launhardt R., Mezger P.G., Haslam C.G.T., Kreysa E., Lemke R., Sievers A., Zylka R., 1996, *A&A* 312, 569
- Launhardt R., Ward-Thompson D., Henning Th., 1997a, *MNRAS* , in press
- Launhardt R., Henning Th., Zylka R., 1997b, in preparation
- Lebrun F., 1986, *ApJ* 306, 16
- Lemme C., Wilson T.L., Tieftrunk A.R., Henkel C., 1996, *A&A* 312, 585

- Leung C.M., 1985, Physical conditions in isolated dark globules. In: Black D.C., Matthews M.S. (eds.), *Protostars and Planets II*. University of Arizona Press, p.104
- Lindblad P.O., Grape K., Sandquist A., Schober J. 1973, *A&A* 24, 309
- Martin R.N., Barrett A.H., 1978, *ApJS* 36, 1
- Men'shchikov A.B., Henning Th., 1997, *A&A* 318, 879
- Meurs E.J. A., Harmon R.T., 1988, *A&A* 206, 53
- Mezger P.G., Chini R., Kreysa E., Wink J., Salter C.J., 1988, *A&A* 191, 44
- Mezger P.G., Sievers A.W., Haslam C.G.T., Kreysa E., Lemke R., Mauersberger R., Wilson T.L., 1992, *A&A* 256, 631
- Morgan J.A., Bally J., 1988, *ApJ* 372, 505
- Mouschovias T.C., 1976, *ApJ* 206, 753
- Neckel T., Chini R., Güsten R., Wink J.E., 1985, *A&A* 153, 253
- Neckel T., Staude H.J., 1990, *A&A* 231, 165
- Nozawa S., Mizuno A., Teshima Y., Ogawa H., Fukui Y., 1991, *ApJS* 77, 647
- Ossenkopf V., Henning Th., 1994, *A&A* 291, 943
- Osterloh M., Beckwith S.V.W., 1995, *ApJ* 439, 288
- Persi P., Ferrari-Toniolo M., Busso M., Origlia L., Robberto M., Scaltriti F., Silvestro G., 1990, *AJ* 99, 303
- Palla F., Stahler S.W., 1990, *ApJ* 360, L47
- Palla F., Galli 1997
- Reipurth B., 1983, *A&A* 117, 183
- Reipurth B., Graham J.A., 1988, *A&A* 202, 219
- Sandquist A., Lindroos K.P., 1976, *A&A* 53, 179
- Sandquist A., Tomboulides H., Lindblad P.O., 1988, *A&A* 205, 225
- Sargent A.I., 1977, *ApJ* 218, 736
- Shu F.H., 1992, *The Physics of Astrophysics, vol II: Gas Dynamics*. Univ. Science Books, Mill Valley, p.360
- Shu F.H., Adams F.C., Lizano S. 1987, *Ann. Rev. Astron. Astrophys.*, 25, 23
- Snell R.L., 1981, *ApJS* 45, 121
- Stahler S.W., 1988, *ApJ* 332, 804
- Stahler S.W., Shu F.H., Taam R.E., 1980, *ApJ* 241, 637
- Stecklum B., Fischer O., Launhardt R., Leinert C., 1997, *A&A* (submitted)
- Terebey S., Shu F., Cassen P.C., 1984, *ApJ* 286, 529, (TSC)
- Terebey S., Chandler C.J., André P., 1993, *ApJ* 414, 759
- Thum C., Kreysa E., John D., Gemünd H.P., Brunswig W., Greve A., Haslam G., Lemke R., Reuter H.P., Ruiz M., Sieveres A., Steppe H., 1992, *A Facility Bolometer for the IRAM 30-m Telescope*. IRAM working report No. 212/92
- Ungerechts H., Thaddeus P., 1987, *ApJS* 63, 654
- Wang Y., Evans II N.J., Zhou S., Clemens D.P., 1995, *ApJ* 454, 217
- Wang Y., Evans II N.J., Launhardt R., Clemens D.P., Henning Th., Yun J.L., 1997, in preparation
- Ward-Thompson, D., Scott, P.F., Hills, R.E., André, P., 1994, *MNRAS* 268, 276
- Wilking B.A., Lada C.J., Young E.T., 1989, *ApJ* 340, 823
- Wouterloot J.G.A., Habing H.J., 1983, *A&A* 151, 297
- Wouterloot J.G.A., Henkel C., Walmsley C.M., 1989, *A&A* 215, 131
- Yun J.L., 1994, *A Characterization of Young Stellar Objects in Bok Globules: Infrared Imaging, Spectral Energy Distributions, and Molecular Outflows*. PhD Thesis, Boston University
- Yun J.L., 1996, *AJ* 111, 930
- Yun J.L., Clemens D.P., 1992, *ApJ* 385, L21
- Yun J.L., Clemens D.P., 1994a, *ApJS* 92, 145
- Yun J.L., Clemens D.P., 1994b, *AJ* 108, 612
- Yun J.L., Clemens D.P., 1995, *AJ* 109, 742
- Zhou S., Evans II N.J., Kömpe C., Walmsley C. M., 1993, *ApJ* 404, 232